Investigating common coding of observed and executed actions in the monkey brain using cross-modal multi-variate fMRI classification.

Prosper Agbesi Fiave[1], Saloni Sharma[1], Jan Jastorff[2], Koen Nelissen[1,*]

Affiliations:

[1]Laboratory for Neuro- & Psychophysiology, Department of Neurosciences, KU Leuven, Leuven, Belgium.

[2]Research Group Psychiatry, Department of Neurosciences, KU Leuven, Leuven, Belgium.

[*]Corresponding author: Koen Nelissen

Address:

Lab for Neuro- & Psychophysiology

O&N2 Campus Gasthuisberg

KU Leuven

Herestraat 49, bus 1021

3000 Leuven, Belgium

Email: Koen.Nelissen@ kuleuven.be

Abstract

Mirror neurons are generally described as a neural substrate hosting shared representations of actions, by simulating or 'mirroring' the actions of others onto the observers' own motor system. Since single neuron recordings are rarely feasible in humans, it has been argued that cross-modal multi-variate pattern analysis (MVPA) of non-invasive fMRI data is a suitable technique to investigate common coding of observed and executed actions, allowing researchers to infer the presence of mirror neurons in the human brain. In an effort to close the gap between monkey electrophysiology and human fMRI data with respect to the mirror neuron system, here we tested this proposal for the first time in the monkey. Rhesus monkeys either performed reach-and-grasp or reach-and-touch motor acts with their right hand in the dark or observed videos of human actors performing similar motor acts. Unimodal decoding showed that both executed or observed motor acts could be decoded from numerous brain regions. Specific portions of rostral parietal, premotor and motor cortices, previously shown to house mirror neurons, in addition to somatosensory regions yielded significant asymmetric, action-specific cross-modal decoding. These results validate the use of cross-modal multi-variate fMRI analyses to probe the representations of own and others' actions in the primate brain and support the proposed mapping of others' actions onto the observer`s own motor cortices.

Keywords: MVPA, fMRI, macaque, mirror neuron, motor

Introduction

Common coding of own and others' actions seems to be a widespread phenomenon in the brain (Jeannerod, 2001; Ebisch et al., 2008; Keysers and Gazzola, 2009; Pulvemüller and Fadiga, 2010; Mooney, 2014; Rizzolatti and Sinigaglia, 2016). In primates, it has been suggested that a special class of visuo-motor neurons, termed mirror neurons (di Pellegrino et al., 1992; Gallese et al., 1996), form the basis of such shared representations, by mapping others' actions onto the observers' own motor system. Although the proposed cognitive function(s) of these mirror neurons and their potential importance for a wide range of social skills and capabilities are still not fully understood (Hickok, 2013; Cook et al., 2014; Bonini, 2016), one current theory suggests that mirror neurons allow simulating observed actions goals onto the same motor goal representations in the own motor system (Gallese et al., 1996; Ferrari et al., 2005; Rochat et al., 2010), and hence provide a straightforward way for understanding or predicting others' actions (Rizzolatti et al., 2001, Rizzolatti and Sinigaglia, 2016).

Since studying the functional responses of individual neurons is not possible in humans except in special cases (but see Mukamel et al., 2010), most studies investigating the human mirror neuron system have employed non-invasive techniques (like fMRI, MEG or EEG) which typically lack the resolution to demonstrate common coding at the single neuron level. The majority of these studies have taken the response of motor cortices to action observation or overlapping responses during action observation and action execution tasks as evidence for the presence (or absence) of mirror neurons (for review Oosterhof et al., 2013; Kilner and Lemon, 2013). This approach has led to the suggestion of an extended human mirror system, even including areas typically considered visual (Caspers et al., 2010, Molenberghs et al., 2012), and extending well beyond those regions previously described in monkeys (Rozzi and Coudé, 2015). However, the validity of this approach has been questioned since these overlapping responses could be caused by 1) general effects of task engagement (different from the baseline condition) not directly related to action observation and execution (Oosterhof et al., 2013); or 2) two discrete populations of neurons with visual and motor properties (Dinstein et al., 2008).

For this reason, other fMRI based methods like fMRI adaptation (Grill-Spector and Malach, 2001) and multi-variate pattern analysis (MVPA) methods (Haxby et al., 2001) have been proposed as more suitable methods for probing the presence of mirror neurons in the human

brain (Etzel et al., 2008; Chong et al., 2008; Dinstein et al., 2008; Lingnau et al., 2009; Kilner et al., 2009; Oosterhof et al., 2010, 2012a, 2013; de la Rosa et al., 2016). The logic behind using cross-modal MVPA as a tool for studying the human mirror neuron system is that patterns of activated voxels associated with executing (or observing) a particular action should be more similar to the pattern elicited by observing (or executing respectively) the same action, when compared to the pattern elicited by a different action. In other words, the underlying assumption is that action-specific cross-modal (vision to motor or vice-versa) decoding is a key feature of regions housing mirror neurons (Oosterhof et al., 2013). So far, however, investigations using cross-modal MVPA to study common coding and the human mirror neuron system have yielded mixed results with respect to showing cross-modal and action-specific effects. While some researchers have failed to find cross-modal action-specific decoding between observed and executed intransitive actions (Dinstein et al., 2008), others have reported cross-modal action-specific decoding between either visual and motor (Oosterhof et al., 2010, 2012a) or auditory and motor domains (Etzel et al., 2008). The aforementioned studies reporting cross-modal action-specific decoding are also inconsistent with respect to the brain regions showing these effects, implementing either parietal, premotor or even occipito-temporal (OT) cortices as loci yielding common coding or shared representations of own and others' actions.

Here for the first time we employed similar cross-modal MVPA methods in rhesus monkeys executing or observing reach-and-grasp and reach-and-touch actions (Fig.1; Supplementary movies 1 to 4). Rhesus monkeys were trained to perform two manual motor acts with their right hand in the MR scanner: a reach-and-grasp movement (grasp execution, GE; Fig.1A,E) or a reach-and-touch movement (touch execution, TE; Fig. 1B,E). Both types of manual motor actions were performed in the dark, to exclude the visual feedback from seeing their own hand during the motor tasks. This ensured that cross-modal decoding (between observed and executed actions) could not be attributed to the mere fact that the monkey saw the same motor act in both cases. In different blocks throughout the fMRI runs, the monkeys were required to fixate on videos showing humans performing similar motor acts (Fig.1C,D,F) as in the execution tasks. These videos consisted of human actors either performing a reach-and-grasp (grasp observation, GO) or a reach-and-touch movement (touch observation, TO).
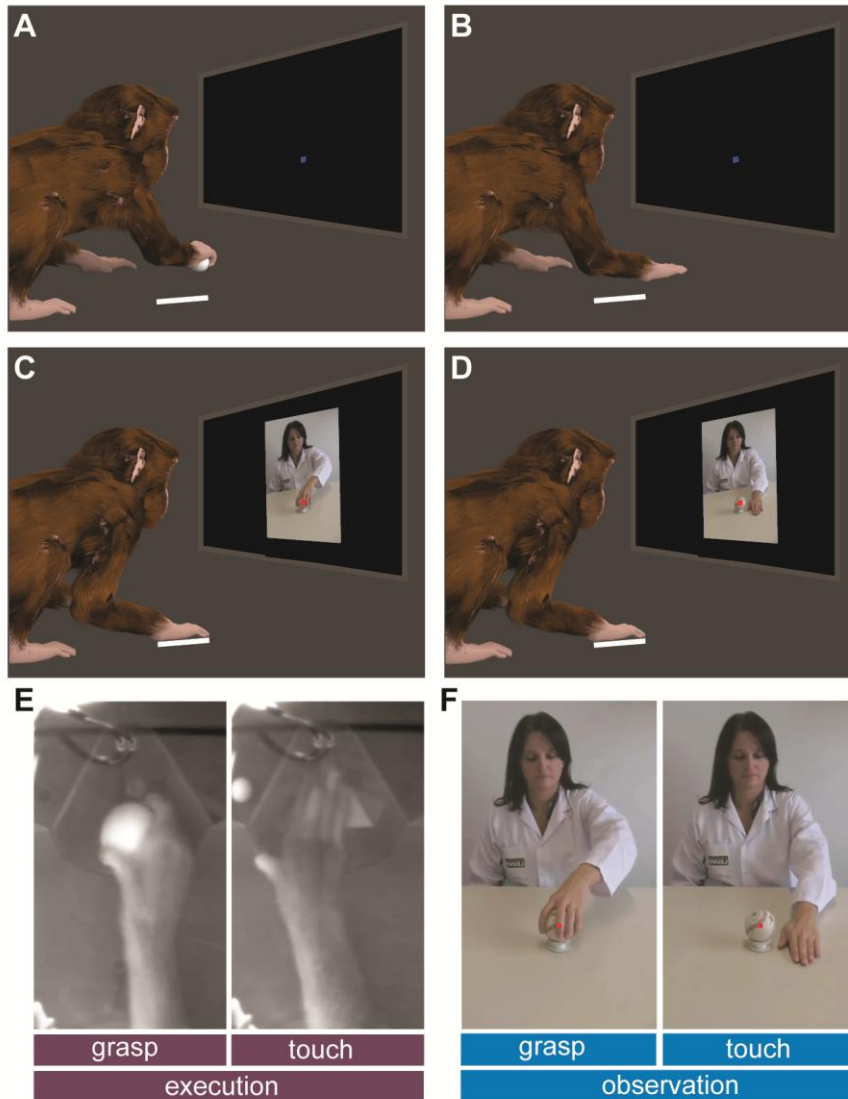
Figure 1. Experimental task design.

A,B. Monkeys were trained to perform either reach-and-grasp (A) or reach-and-touch (B) actions in the dark in the MR scanner, while being cued on a screen placed in front of them.

C,D. During different blocks in the same fMRI runs, monkeys also observed videos of human actors performing similar reach-and-grasp (C) or reach-and-touch (D) actions, while keeping their hand in the start position (indicated with a white line).

E. Example of a reach-and-grasp (left panel) and reach-and-touch (right panel) action executed by a monkey in the scanner.

F. Frame of two action observation videos, depicting a human actor performing either a reach-and-grasp (left panel) or a reach-and-touch (right panel) action. Red dot superimposed on the object in the video indicates fixation target.

As a proof-of-principle, we examined in particular if key regions of the parieto-frontal mirror neuron system (parietal area PFG and premotor F5c) showed action-specific cross-modal representations that could be retrieved by means of cross-modal MVPA of fMRI data. In addition, since more recent electrophysiological studies in monkeys have also suggested the presence of grasping-related mirror neurons or mirror-like responses in additional regions like parietal area AIP, primary motor cortex F1 (or M1), dorsal premotor and ventrolateral prefrontal cortices, we also investigated whether these regions yielded action-specific cross-modal decoding. Finally, since several human fMRI studies have suggested shared representations for own and others' actions also in somatosensory cortices and in the OT complex (Keysers et al., 2010; Oosterhof et al., 2010, 2013), we also included the presumed monkey homologues of these regions in the analysis. Importantly, performing these studies in rhesus monkeys allowed us to directly test the assumptions behind this non-invasive technique on brain regions known to house mirror neurons, which is not feasible in humans.

Material and Methods

Subjects

Two male (M1, M2) rhesus monkeys (*Macaca mulatta*, 4-6 kg, 3-5 years old) participated in the experiments. All animal care and experimental procedures met the national and European guidelines and were approved by the animal ethical committee of the KU Leuven. The details of the surgical procedures, training of monkeys, image acquisition, eye monitoring and statistical analysis of monkeys scans have been described previously (Vanduffel et al., 2001; Nelissen et al., 2005; Nelissen et al., 2011; Nelissen et al., 2017).

Functional MRI fixation training

The subjects were trained to sit in a sphinx position in a plastic monkey chair (Suppl. Fig. 1A, 1). Training took place in a mock scanner, while the subjects were directly facing a liquid crystal display (LCD) screen (Suppl. Fig. 1A, 5), which was positioned at 53 cm from the monkeys` eyes. During initial training they were required to maintain fixation within a 2x2°

window centered on a red dot (0.35 x 0.35°) in the middle of the screen. Eye position was monitored at 120Hz (Suppl. Fig. 1A, 6) through pupil position and corneal reflection (Iscan). During this training phase, the monkeys were rewarded with drops of fruit juice for fixating within the fixation window for long periods of time (often up to several minutes).
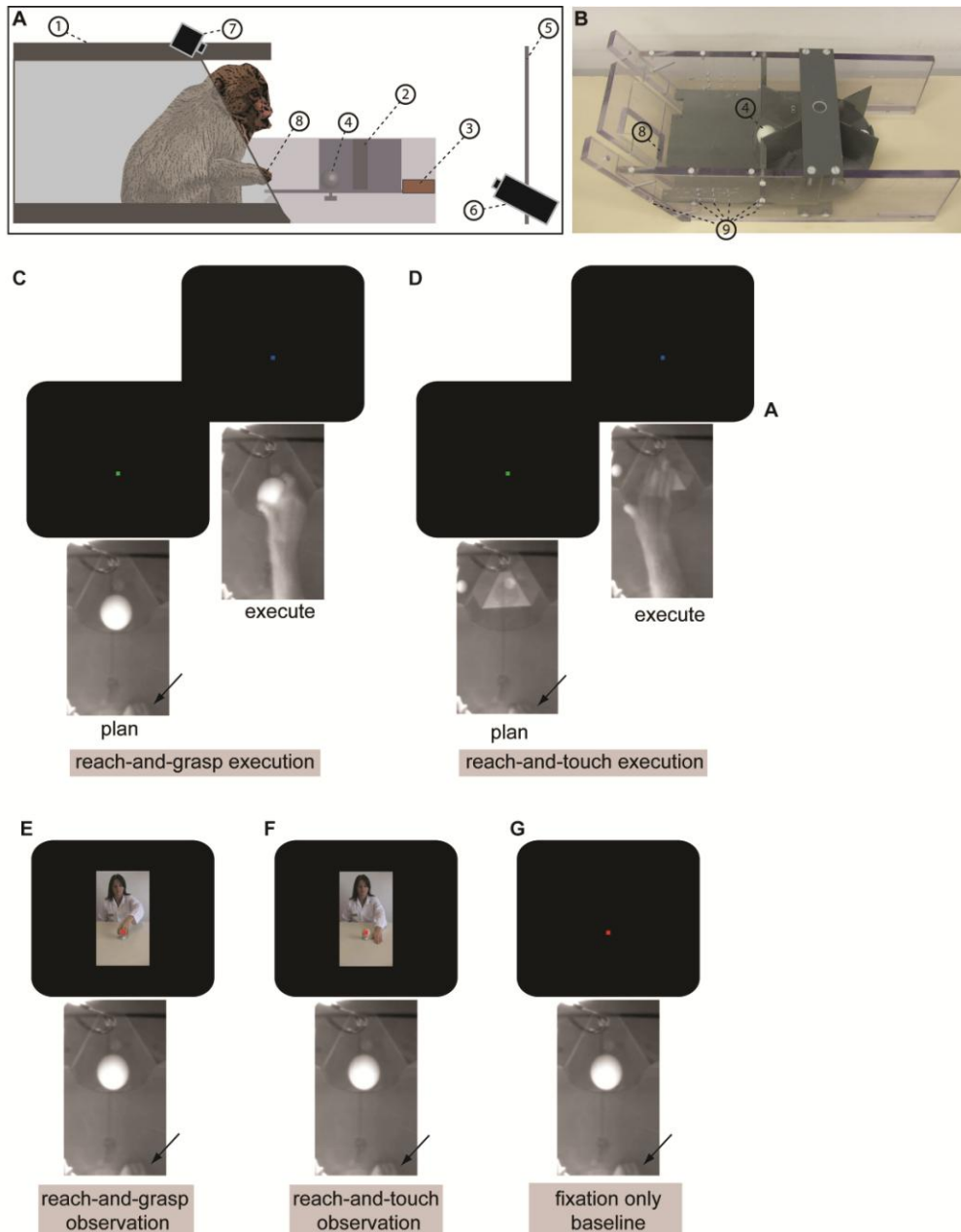
Supplementary Figure 1. Monkey fMRI experimental setup for motor and visual tasks.

A. During the fMRI experiments, monkeys were seated in an MR-compatible chair (1). A rotating carousel (2) was attached to the front of the chair and powered by an MR-compatible motor (3), which allowed a graspable object (4)

or an empty space (no object present) to be positioned in front of the monkey. Monkeys performed either reach-and-grasp or reach-and-touch actions in the dark without visual feedback, while being cued on a screen in front of them (5). Eye movements (6) and hand movements (7) were monitored using MR-compatible cameras.

B. At the hand start position (8) and at different places along the reach trajectory (9), optic fibers were positioned in order to track the hand position of the monkey during the scans.

C,D. During the action execution tasks, monkeys were cued with small fixation points presented on the screen in front of them (see methods). At the beginning of a trial monkeys kept their hand in the start position (black arrow), while a green fixation dot was presented on the screen in front of them. When the color changed to blue, they could reach forward and grasp the object (grasping trial, C) or place their open right hand on the empty slot on the disk (touch trial, D) to receive a juice reward. Breaking of fixation or incorrect motor behavior would result in a trial abort during which a small yellow cross was presented on the screen (see methods).

E, F. During the action observation tasks, monkeys fixated a red dot presented on the screen in front of them, while videos of human actors performing reach-and-grasp (E) or reach-and-touch actions (F) were presented. Monkeys were rewarded for keeping fixation while keeping their right hand in the start position (black arrow, E, F)

G. During fixation-only baseline blocks, monkeys received juice rewards for fixating a red dot and keeping their right hand in the start position (black arrow).

Visual stimuli

The visual stimuli consisted of video clips showing human actors performing two different actions: a *reach-and-grasp* or a *reach-and-touch* action (Fig. 1F). Supplementary Video 3 and Supplementary Video 4 show one example of respectively, a *reach-and-grasp* and a *reach-and-touch* action video. In total, eight different *reach-and-grasp* and *reach-and-touch* videos each were used: two female actors either grasped 4 different objects or placed their open hand next to these objects (Suppl. Fig. 2). This ensured there was some variation in 1) the actor, 2) the object and 3) the movement kinematics across the videos, while keeping the goal of the two types of videos constant: grasp or touch. In the *reach-and-touch* videos (Fig.1F; Suppl. Fig. 2B), the objects were always visible, in order to exclude the possibility that classification between the two visual conditions might be driven (partly) by the presence or absence of a graspable object in the video, which might modulate activity in parietal and premotor motor regions (Rizzolatti and

Fadiga, 1998; Murata et al., 2000). The size of the videos was 8.5 x 14 visual degrees. The duration of each video was 4 seconds. Thus, during a typical grasp observation or touch observation block which lasted 32 seconds in total, each of the eight videos would be presented once in a random order.
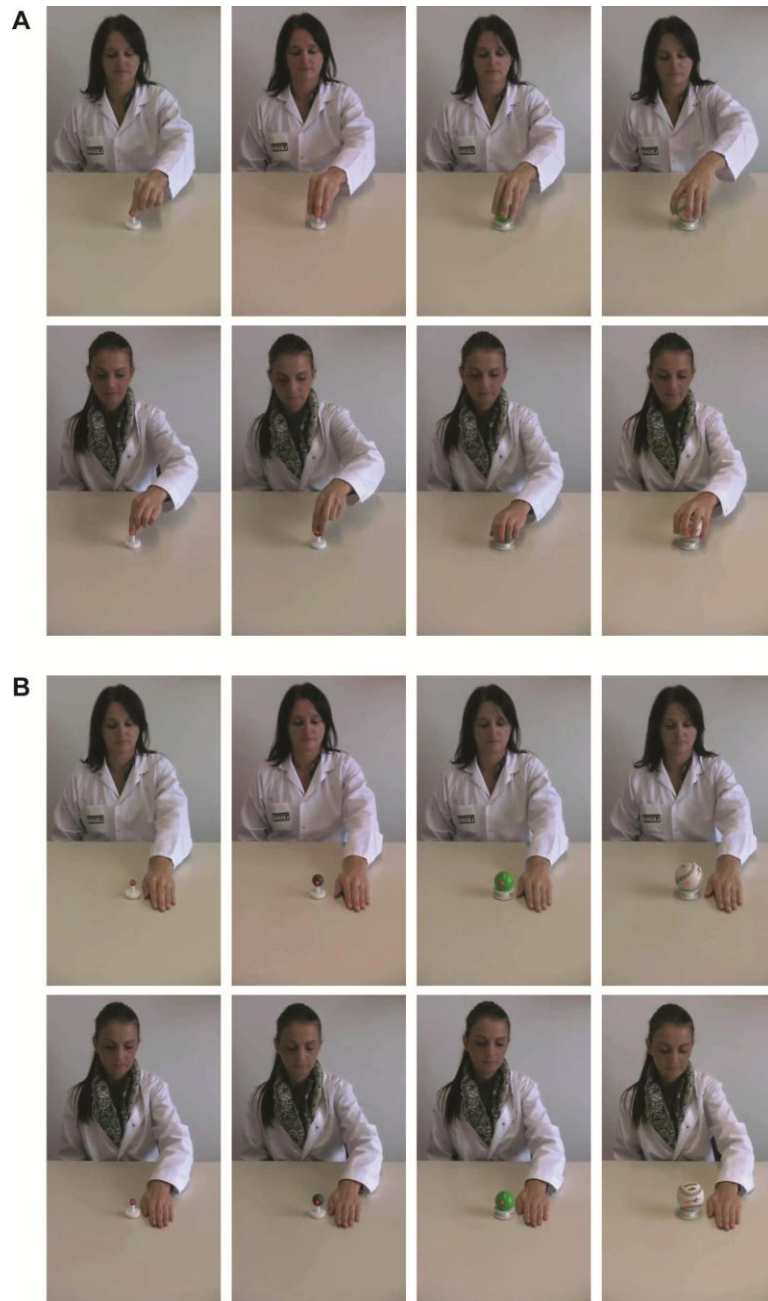
Supplementary Figure 2. Videos of human actors performing reach-and-grasp and reach-and-touch actions.

A. Reach-and-grasp action videos consisted of two female actors, each grasping 4 different sized objects.

B. Reach-and-touch action videos consisted of the same actors, each reaching forward and placing their hand with an open palm next to these objects.

Motor tasks

The subjects were trained to perform two different manual motor acts: a *reach-and-grasp* movement (Fig. 1A,E; Suppl. Fig. 1C) or a *reach-and-touch* movement (Fig. 1B,E; Suppl. Fig. 1D). Supplementary Video 1 and Supplementary Video 2 show one example of respectively, a *reach-and-grasp* and a *reach-and-touch* motor act performed by a monkey. For both motor tasks, we used a custom-built MR-compatible turntable (Nelissen and Vanduffel, 2011; Nelissen et al., 2017). The turntable (Suppl. Fig. 1A, 2; Suppl. Fig. 1B) could be rotated through a gear and belt system, powered by an MR-compatible pneumatic stepper motor (Suppl. Fig. 1A, 3; Stoianovici et al., 2007). This system was computer controlled and was triggered by the scanner. The disk could rotate with a speed of 15 degrees per second. One of the slots on the rotating disk held a 3 cm diameter sphere (Suppl. Fig. 1A, 4; Suppl. Fig. 1C), while another empty slot on the disk (Suppl. Fig. 1D) was used for the reach-and-touch task. The sphere was connected through a shaft to a small plastic weight below the disk (Suppl. Fig. 1A, 4). This allowed the object to fall back into place once the subject released it after completing the grasping movement. Both motor tasks were performed in the dark, to avoid neural modulations due to visual feedback from the hand and arm or the object. During the first trial of a motor block, the subject reached forward and felt the presence or absence of the object in front of him. Subsequently, the subject would either continue to grasp the object or to place his open hand on the empty disk, for the remainder of the trials in that particular motor block (Nelissen and Vanduffel, 2011; Nelissen et al., 2017). In each fMRI run, the subjects would perform the two motor tasks in blocks of 32 seconds. In any given motor block, approximately 7 to 8 motor actions (either reach-and-grasp or reach-and-touch) were performed.

For the *reach-and-grasp* task, a trial started when the monkey placed his hand in the start position (Suppl. Fig. 1A, 8; Suppl. Fig. 1C, black arrow) and fixated on a green fixation point displayed centrally on the screen in front of him (Suppl. Fig. 1C). If the monkey removed his hand or stopped fixating before a certain random time (varying between 500 ms and 1500 ms), the trial was aborted and a yellow cross was displayed until the monkey again placed his hand at the starting position (Nelissen and Vanduffel, 2011; Nelissen et al., 2017). After a variable

fixation time (between 500 to 1500 ms), the green fixation point changed to blue, indicating to the monkey that he could now reach and grasp the object with its right hand (Suppl. Fig. 1C). Trials where the subject failed to grasp the object within 2000 ms were immediately aborted. After the monkey had grasped the object, he was required to lift it 5 mm and hold it in that position for at least 530 ms (maximum holding time 2000 ms) to receive a juice reward. After delivery of the reward, a new trial started (green fixation point) as soon as the monkey returned his hand to the initial starting position while keeping fixation. At the hand start and end positions of the reaching trajectory, as well as at three locations along this hand/arm trajectory, optic fiber cables were positioned (Suppl. Fig. 1B, 9), which allowed us to track the location of the monkeys` hand/arm and to record the timing of the execution of the motor tasks (Nelissen and Vanduffel, 2011).

During the *reach-and-touch* task, the disk was rotated so that an empty slot that did not contain an object was positioned in front of the monkey (Suppl. Fig. 1D). The monkey was required to reach forward and place his open hand on the disk (Suppl. Fig. 1D). The visual signals used to cue the monkey and the timing parameters were exactly the same for the reach-and-grasp task as they were for the *reach-and-touch* task. The monkey was required to leave his open hand on the disk for at least 530 ms in order to receive the juice reward. As for the *reach-and-grasp* task, optic fibers monitored the position of the hand.

Visual tasks

During different blocks in the same fMRI runs, monkeys also observed videos of human actors performing *reach-and-grasp* (Fig. 1F, Suppl. Fig. 1E) or *reach-and-touch* (Fig. 1F, Suppl. Fig. 1F) actions. During these visual blocks, which lasted 32 seconds each, monkeys were rewarded for fixating a red fixation spot while videos were being displayed on the screen. During these action observation fixation blocks, monkeys were required to keep their right hand in the start position (Suppl. Fig. 1E,F, black arrow). Finally, during a fixation baseline condition, monkeys were rewarded for fixating on a red fixation point only (Suppl. Fig. 1G), while keeping their right hand in the start position (Suppl. Fig. 1G, black arrow). In case subjects broke fixation or removed the hand from the start position during the visual blocks, reward delivery would immediately be stopped and a small yellow cross would be presented instead of the red fixation target. Performance during the fMRI tasks was monitored using both optic fibers (Suppl. Fig.1B,

see Methods) and an MR compatible camera (MRC Systems, Heidelberg, Germany, see Nelissen and Vanduffel, 2011; Nelissen et al., 2017).

Scanning

Functional images were acquired with a 3.0 Tesla full-body scanner (Siemens), using a gradient-echo T2*-weighted echo-planar imaging sequence (40 horizontal slices; TR, 2 s; TE, 17 ms; 1.25 x 1.25 x 1.25 mm^3 isotropic voxels) with a custom built eight-channel phased-array receive coil, and a saddle-shaped, radial transmit-only surface coil (Kolster et al., 2009).

Before each subject`s scanning session, a contrast agent, monocrystalline iron oxide nanoparticle (MION), was injected into the femoral/saphenous vein (6-11mg/kg). The contrast agent improved the contrast-noise ratio approximately fivefold (Vanduffel et al., 2001) and enhanced spatial selectivity of the magnetic resonance (MR) signal changes (Zhao et al., 2006), compared to blood oxygenation level-dependent (BOLD) measurements. While BOLD measurements depend on cerebral blood volume (CBV), blood flow, and oxygen extraction, MION measurements depend only on blood volume (Mandeville et al., 1999). Herein, we have inverted the polarity of all signal-change values to account for the difference between MION CBV and BOLD activation maps (i.e. increased brain activation produces a decrease in MR signal in MION CBV maps).

We used a block design, with alternating blocks (or epochs) of fixation only, reach-and-grasp execution (GE), reach-and-touch execution (TE), reach-and-grasp observation (GO) and reach-and-touch observation (TO). Each epoch consisted of 16 volumes (32 seconds). A complete run totalled 9 min and 14 seconds, during which 277 whole-brain volumes were acquired. A typical run consisted of 5 volumes of fixation only – 16 volumes fixation only - 16 volumes GO – 16 volumes fixation only - 16 volumes TO – 16 volumes fixation only - 16 volumes GE – 16 volumes fixation only - 16 volumes TE – 16 volumes fixation only - 16 volumes GO – 16 volumes fixation only - 16 volumes TO – 16 volumes fixation only - 16 volumes GE – 16 volumes fixation only - 16 volumes TE – 16 volumes fixation only. In total, 4 different orders were used during the fMRI experiments in both monkeys, two of which that started with the visual conditions (GO – TO – GE – TE and GO – TO – TE – GE) and two orders that started with the motor conditions (GE – TE – GO – TO and TE – GE – GO – TO). A total of

20 runs from each subject were used for the multi-voxel pattern analysis, acquired in 4 separate fMRI sessions for monkey M1 and in 2 separate fMRI sessions for monkey M2.

Behavioral performance during fMRI runs

Monkey M1 made on average 13,55 reach-and-grasp movements and 14,75 reach-and-touch movements per run. Monkey M2 made on average 16,95 reach-and-grasp movements and 16,55 reach-and-touch movements per run. Eye movement analysis showed that there was no significant difference in fixation performance between both action execution conditions in either of the 2 monkeys (monkey M1: on average 5,7 saccades/min during both the reach-and-grasp motor task and the reach-and-touch motor task, $p = 0.083$; monkey M2: on average 3,9 saccades/min during the reach-and-grasp motor task and 5,8 saccades/min during the reach-and-touch motor task, $p = 0.054$). In addition, no difference was found in fixation performance for the action observation conditions in either of the 2 monkeys (monkey M1: on average 5,8 saccades/min during both the reach-and-grasp observation condition and the reach-and-touch observation condition, $p = 0.276$; monkey M2: on average 3,8 saccades/min both during the reach-and-grasp observation condition and the reach-and-touch observation condition, $p = 1$).

Definition of Regions-of-Interest (ROIs)

Since monkeys were trained to perform the motor acts with their right hand and the actions depicted in the videos were presented with a bias to the right visual field, we focussed in particular on ROIs in the left (contralateral) hemisphere. In total, we delineated 12 different ROIs in the contralateral left hemisphere (black outlines in Fig. 2). The corresponding ROIs in the right hemisphere are shown in Suppl. Fig.3. Each ROI was selected on the basis that it had previously been shown to either a) house mirror neurons, or b) to be involved in action execution and/or action observation. ROIs were delineated manually using FSL (v5.0), directly onto a template monkey anatomical MR image (M12 from Ekstrom et al., 2008), guided by anatomical landmarks and based upon previous anatomical and functional studies, as described in detail for each individual ROI below. This procedure of manually selecting voxels directly on consecutive anatomical MR slices was to ensure that voxels were located mainly in the grey matter and to avoid the inclusion of unwanted voxels (for instance on the opposite bank of a sulcus close to a local maximum).

In the *rostral parietal cortex*, we defined a ROI for area PFG on the inferior parietal convexity and another ROI for anterior intraparietal area AIP in the lateral bank of the intraparietal sulcus (Fig.2). Parietal mirror neurons related to prehension movements have been demonstrated particularly in area PFG (Fogassi et al., 2005; Rozzi et al., 2008), but more recently neurons responding during grasping execution and observation have also been observed in area AIP (Pani et al., 2014). Delineating these parietal ROIs was based upon previous single-cell (Rozzi et al., 2008; Murata et al., 2000; Gregoriou et al., 2006) and fMRI studies (Durand et al., 2007; Nelissen et al., 2011). The posterior border of AIP with the lateral intraparietal area (LIP) was derived in a previous fMRI study (Durand et al., 2007), using the same anatomical MR template as in our study and an eye movement task that yielded saccadic responses in LIP, but not AIP (Durand et al., 2007).

In *ventral premotor cortex*, guided by anatomical landmarks, we delineated a ROI for area F5c located on the convexity, as well as two additional ROIs in the posterior bank of the arcuate sulcus, corresponding to F5p and F5a (Nelissen et al., 2005; Belmalih et al., 2009; Gerbella et al., 2011). While all three ventral premotor F5 sectors have been shown to play a role in different aspects of visuo-motor transformations for grasping and are strongly connected to the parietal nodes of the grasping network, mirror neurons have been recorded mostly in area F5c.

Neurons with mirror-like properties has also been described in different sectors of the *dorsal premotor cortex* (Cisek and Kalaska, 2004; Tkach et al., 2007; Yoshida et al., 2011). Therefore, we also defined a ROI based upon anatomical landmarks (Rizzolatti and Luppino, 2001) for dorsal premotor area F2 and pre-supplementary motor area F6.

In *motor cortex*, we defined a ROI for the hand representation of primary motor cortex (F1 or M1) based on anatomical landmarks (Rizzolatti and Luppino, 2001; Maranesi et al., 2012) and functional responses during active grasping tasks in previous monkey fMRI studies (Nelissen and Vanduffel, 2011; Nelissen et al., 2017). This region plays a pivotal role in the execution of different motor acts, and more recently mirror responses were also demonstrated in this region (Dushanova and Donoghue, 2010; Vigneswaran et al., 2013).

In *prefrontal cortex*, we defined a ROI deemed *vlPF* (ventrolateral prefrontal) which was centered around area 46v and adjacent cortex. A previous fMRI study showed that this area in monkeys responded during action observation (Nelissen et al., 2005), and this converges with recent single-cell and imaging data suggesting both action observation (Simone et al., 2017;

Raos and Savaki, 2016b) as well as movement-related activity during goal-directed hand actions (Simone et al., 2015; Bruni et al., 2015; Raos and Savaki, 2016b) are encoded in this brain region. Based on the aforementioned functional as well as on anatomical data (Gerbella et al., 2013), it has recently been argued that this portion of the brain might house mirror regions (Bonini, 2016). This assertion was supported by the observations of Simone and co-authors (2017) who reported that a small proportion (9/77; 12%) of the recorded neurons in that area that were tested for motor and visual responses also displayed mirror neuron properties. Interestingly, this region was recently also shown to house neurons representing both own and other agents' spatial action goals (Falcone et al., 2016).

Given their potential involvement in the somatosensory or motor aspects of simulation in humans (for review, see Keysers et al., 2010), we also examined ROIs for *primary (SI)* and *secondary (SII) somatosensory cortices*. These somatosensory ROIs were delineated on the anatomical template, based on anatomical landmarks and functional responses during passive and active tactile stimulation experiments performed previously in both monkey subjects (Nelissen and Vanduffel, 2011; Sharma et al., 2018). The ROI for *SI* corresponded mostly to portions of areas 3b, 1 and 2. The ROI for *SII* corresponded to the more anterior portion of SII that yielded visual and motor-related responses in the study of Sharma et al. ('visual SII' of Sharma et al., 2018).

Finally, we defined a ROI that is hereafter referred to as *mSTS* (middle STS), this ROI includes areas MT and FST (Nelissen et al., 2006), as well as the monkey posterior STS body patch (Popivanov et al., 2012); the body patch being a potential homologue of human EBA (Caspari et al., 2014). The rationale for defining this ROI was that it corresponds, at least in part, to portion of occipito-temporal (OT) cortex in humans that has been investigated in studies of action recognition (Wurm and Lingnau, 2015) and common coding of observed and executed actions (Oosterhof et al., 2013). This human OT cluster that yields both univariate and multi-variate cross-modal responses during action execution and observations tasks is thought to contain several functionally distinct regions including human middle temporal area (MT) complex and the extrastriate body area (EBA; Oosterhof et al., 2010, 2012a). Single cell and imaging data have previously shown that this portion of monkey STS responds to observation of actions (Perret et al., 1989; Nelissen et al., 2006) and may pass visual information about actions to the mirror neuron system (Nelissen et al., 2011; Giese and Rizzolatti, 2015).

Table 1 indicates the number of voxels contained in each of the ROIs.

ROI	Left hemisphere	Right hemisphere
AIP	136	136
PFG	158	158
F5c	301	301
F5p	81	81
F5a	123	123
F2	403	403
F6	277	277
F1	302	302
vIPF	193	193
SI	177	177
SII	65 (M1), 120 (M2)	65 (M1), 120 (M2)
mSTS	244	244

Table 1. Number of voxels in each of the ROIs.

Data Preprocessing and GLM fitting

The raw functional scans were 3D motion-corrected by re-aligning all the volumes to the first volume of the first run of the functional scans using SPM12. To account for the differences in inter-subject anatomy, the realigned functional scans of the two monkeys were warped to match the same high-resolution anatomical scan (M12 anatomical template, using BrainMatch software or JIP). The monkey functional volumes were then subsampled to 1 mm^3. For the univariate analyses shown in Fig. 2, data were further smoothed with an isotropic Gaussian kernel (full width at half height, 1.5 mm). For the multi-variate analyses (see next paragraph), unsmoothed data were used. The response amplitude at each voxel was estimated using a general linear model (GLM) following previously detailed procedures (Friston et al., 1995; Vanduffel et al., 2001). To do this, a MION hemodynamic response function was convolved with a boxcar model representing the various stimulus conditions (Vanduffel et al., 2001). The influence of head motion was accounted for by including in the GLM model six regressors of no interest corresponding to three rotations and translations along x, y and z axis. For each run, a GLM was

fitted for each voxel resulting in a map (beta map) for each condition of interest and the six regressors of no interest. The computed beta maps were next used in the ROI MVPA procedure.

ROI MVPA

For the multi-voxel pattern analysis (MVPA), we used a Matlab-based Decoding Toolbox (Hebart et al., 2015). The extracted beta value of each voxel of the ROI served as input to a linear support vector machine (SVM) with a cost parameter (c=1). We used a leave-one-run-out cross-validation scheme, where at each iteration the data from 19 runs were used to train the classifier and the data from 1 run were left out for testing. For a given ROI, the individual classification performances from 20 iterations (ensuring that each run served as the test data once) were averaged to determine the overall classification performance. This cross-validation scheme minimizes the chance of overfitting the classifier and ensures generalization to previously unseen data. To determine statistical significance of the ROI classification results, we performed permutation analysis where the conditions associated with each feature were randomly shuffled. This procedure was repeated 2000 times. The same cross-validation classification scheme detailed above was applied to classify the data from each dataset, leading to 2000 classification performance values. Based on the classification performance of the permutated data and that of the original classification, p-values were calculated. The p-values were corrected for the number of ROIs using false discovery rate (FDR). ROIs with p-values less that 0.05 after FDR correction were declared significant (indicated with black asterisks in figures). In addition, ROIs with p-values less that 0.05 without correction are indicated with red asterisks in figures.

Within a given ROI, we performed within-modality classification and cross-modality classification. Within-modality classification (Fig.3, Suppl. Fig.4) involves using data extracted from similar modalities (i.e. grasp observation and touch observation or grasp execution and touch execution) for both training and testing a classifier. Cross-modality classification (Fig.4, Suppl. Fig.5) tested cross-modal action-specificity by using the data from one modality for training the classifier and data from the different modality for testing. To determine the influence of the direction of training (Kaplan et al., 2015), we looked at classifier performance when we trained on visual data and tested on motor data, separately from when we trained the classifier on motor data and tested on visual data.

Results

Figure 2 shows the univariate fMRI responses (fixed-effect group result, $p < 0.05$, corr.) in the contralateral (left) hemisphere when monkeys either performed the reach-and-grasp (A) or the reach-and-touch (B) motor acts, or observed the videos of humans performing similar reach-and-grasp (C) or the reach-and-touch (D) actions. Location of the ROIs that were examined in the unimodal and cross-modal multi-variate analyses are shown as black outlines. In line with previous monkey fMRI motor experiments (Nelissen and Vanduffel, 2011), execution of reach-and-grasp or reach-and-touch actions in the dark with the right hand yielded much stronger fMRI responses in the contralateral (Fig.2A,B) compared to the ipsilateral (Suppl. Fig.3A,B) hemisphere. In general, execution of both types of motor acts (compared to fixation only baseline), yielded strongest responses in anterior parietal, motor, somatosensory and frontal cortices (Fig.2A,B). Observing videos of humans performing similar actions (compared to fixation only baseline) yielded significant responses in particular in early visual, extrastriate, STS, parietal and frontal cortices (Fig.2C,D). Total number of significantly ($p < 0.05$, corr.) activated voxels throughout the whole brain in the two action execution and two action observation contrasts (versus fixation only baseline) are shown in Suppl. Table 1.
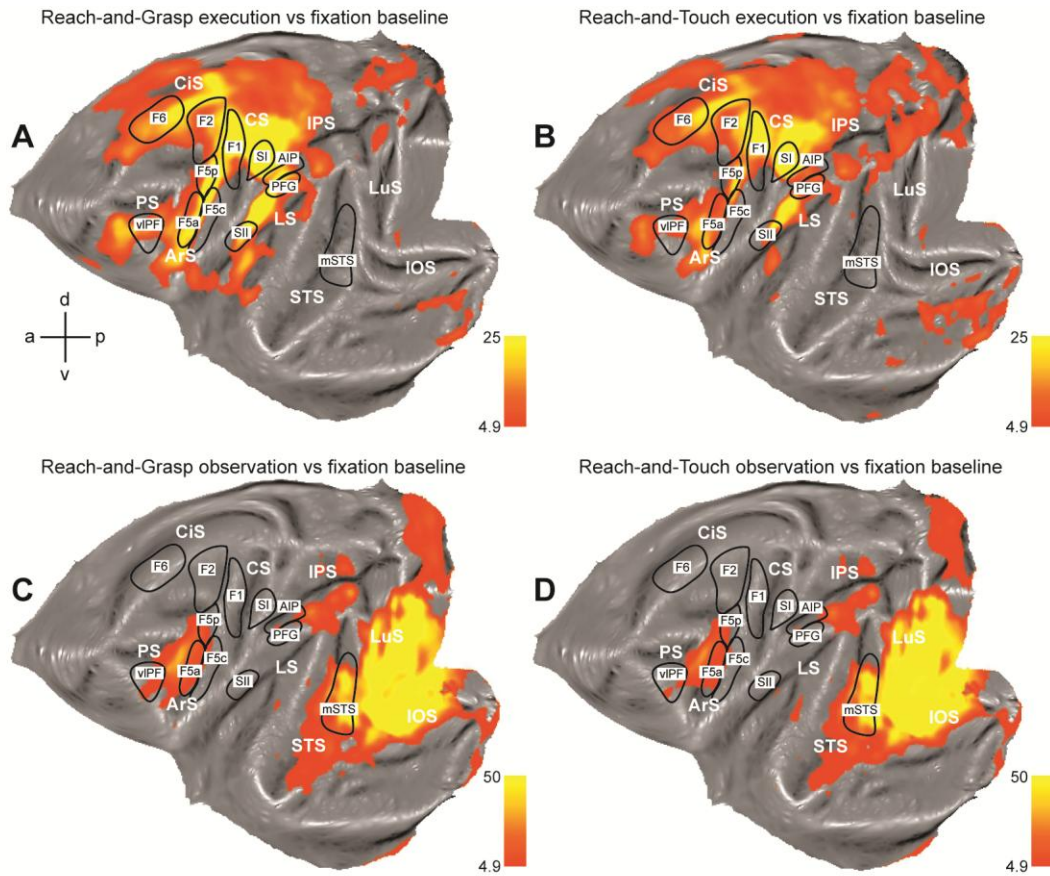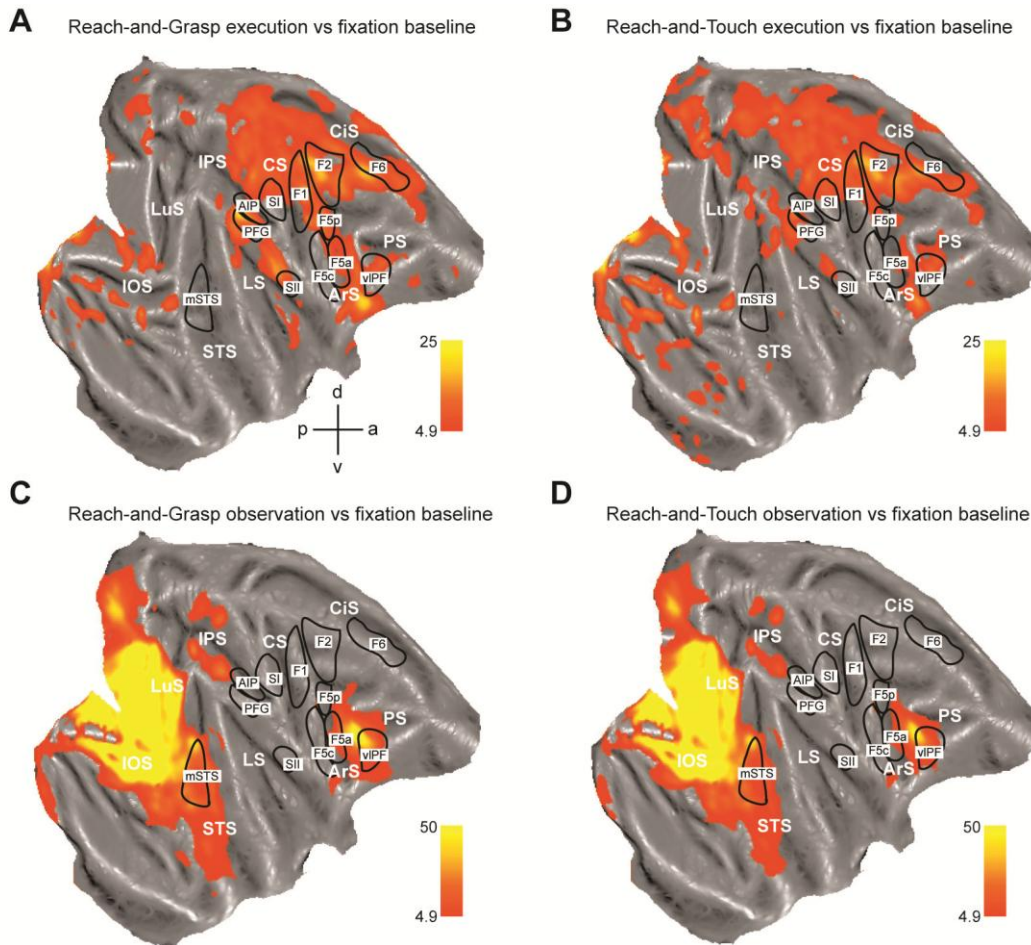
Figure 2. Univariate fMRI responses during action execution and action observation tasks.

Flat maps showing univariate fMRI activations (p < 0.05, corr.; fixed-effects group results) during reach-and-grasp execution (A), reach-and-touch execution (B), reach-and-grasp observation (C) and reach-and-touch observation (D), overlaid on the left hemisphere of anatomical monkey template. Black outlines indicate regions-of-interest (ROIs) examined in this study: middle Superior Temporal Sulcus (mSTS), area PFG in the anterior portion of the inferior parietal lobule, area AIP in the anterior portion of the lower bank of the intraparietal sulcus, primary (SI) and secondary (SII) somatosensory region, hand field of primary motor cortex F1, ventral premotor areas F5c, F5p and F5a, dorsal premotor area F2, supplementary motor area F6 and portion of ventrolateral prefrontal (vlPF) cortex, centered around area 46v. a = anterior, p = posterior, d = dorsal, v = ventral, LuS = lunate sulcus, IOS = inferior occipital sulcus, IPS = intraparietal sulcus, STS = superior temporal sulcus, LS = lateral sulcus, CS = central sulcus, CiS = cingulate sulcus, ArS = arcuate sulcus, PS = principal sulcus.

Supplementary Figure 3. Univariate fMRI responses during action execution and action observation tasks.

Flat maps showing univariate fMRI activations (p < 0.05, corr.; fixed-effects group results) during reach-and-grasp execution (A), reach-and-touch execution (B), reach-and-grasp observation (C) and reach-and-touch observation (D), overlaid on the right (ipsilateral) hemisphere of anatomical monkey template. Black outlines indicate regions-of-interest (ROIs) examined in this study: middle Superior Temporal Sulcus (mSTS), area PFG in the anterior portion of the inferior parietal lobule, area AIP in the anterior portion of the lower bank of the intraparietal sulcus, primary (SI) and secondary (SII) somatosensory region, hand field of primary motor cortex F1, ventral premotor areas F5c, F5p and F5a, dorsal premotor area F2, supplementary motor area F6 and portion of ventrolateral prefrontal (vlPF) cortex, centered around area 46v. a = anterior, p = posterior, d = dorsal, v = ventral, LuS = lunate

sulcus, IOS = inferior occipital sulcus, IPS = intraparietal sulcus, STS = superior temporal sulcus, LS = lateral sulcus, CS = central sulcus, CiS = cingulate sulcus, ArS = arcuate sulcus, PS = principal sulcus.

Next we examined whether at the voxel population level, different motor acts that were either executed or observed could be discriminated based upon their fMRI voxel patterns in the different ROIs (Fig.3A,B). For this, decoders were constructed by training linear support vector machines with fMRI data (Haxby et al., 2001; Norman et al., 2006) while monkeys either performed with their right hand the two different motor acts (reach-and-grasp or reach-and-touch) or observed videos of humans performing similar actions. Consistent with their proposed role in coding prehension motor acts (Borra et al., 2017; Rozzi and Coudé, 2015; Nelissen and Vanduffel, 2011), executed grasps versus touches yielded significantly (p < 0.05, corr.) distinct multi-voxel patterns in contralateral cortex and could be decoded accurately in both monkey subjects in parietal areas AIP and PFG, ventral premotor areas F5c and F5a, primary motor (F1) cortex and dorsal premotor cortex F2 (Fig. 3A,B). In addition, multi-voxel fMRI patterns related to both motor acts allowed significant (p < 0.05, corr.) above-chance classification in ventrolateral prefrontal cortex (vlPF), as well as in secondary (SII) somatosensory cortex in both subjects (Fig.3A,B). Finally, ventral premotor F5p, dorsal premotor F6 and SI ROIs, only yielded significant decoding for both motor acts in one of the two subjects. Results of unimodal decoding of both motor acts in the ipsilateral hemisphere are shown in Suppl. Fig.4A,B.

A second binary classifier examined the representation of observed grasp or touch movements in the same ROIs. As it was for the motor modality, multi-voxel patterns from the majority of examined regions in left hemisphere allowed significant (p < 0.05, corr.) decoding for observed grasps versus observed touch actions (Fig.3C,D). Both types of observed actions could be discriminated based upon their voxel patterns in both subjects in parietal areas AIP and PFG, ventral premotor F5c and F5a, vlPF, SII and mSTS. In 1 of the two subjects, F5p and F1 in addition also allowed significant decoding of the two types of observed actions (Fig. 3D). Results of unimodal decoding of both observed actions in the right hemisphere are shown in Suppl. Fig.4C,D.
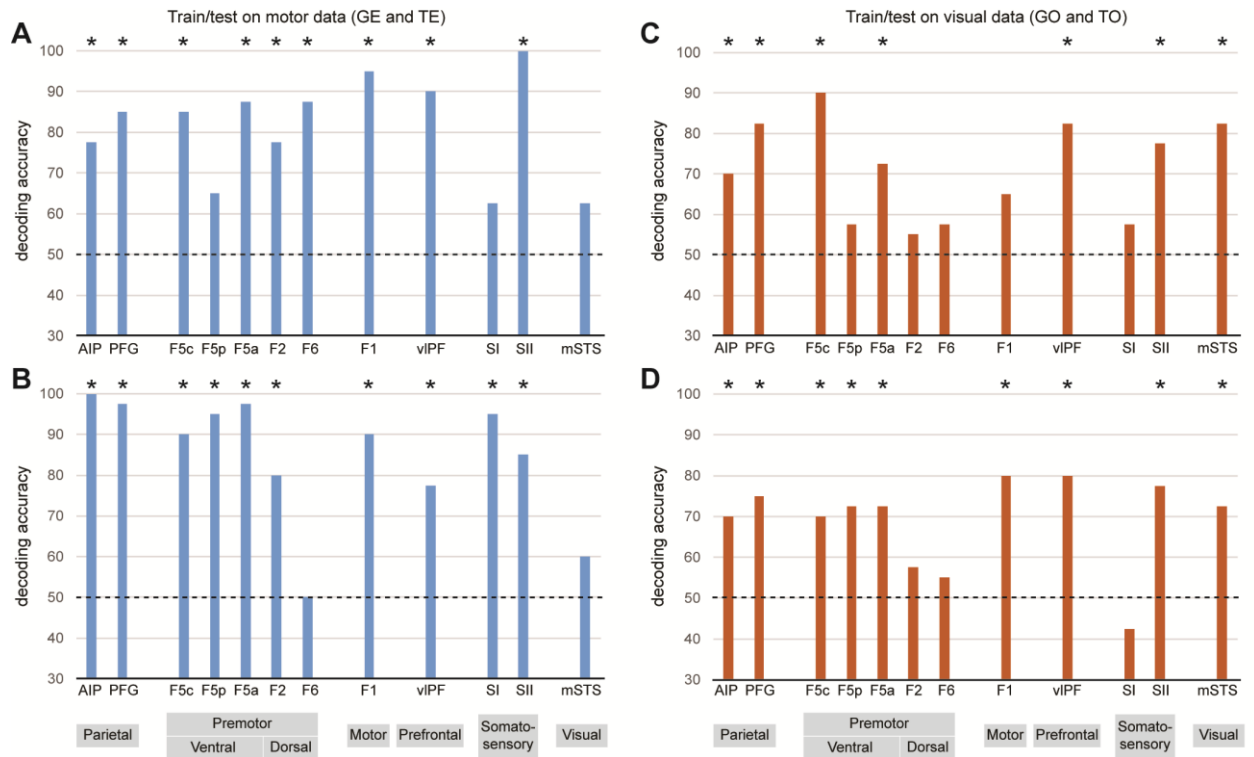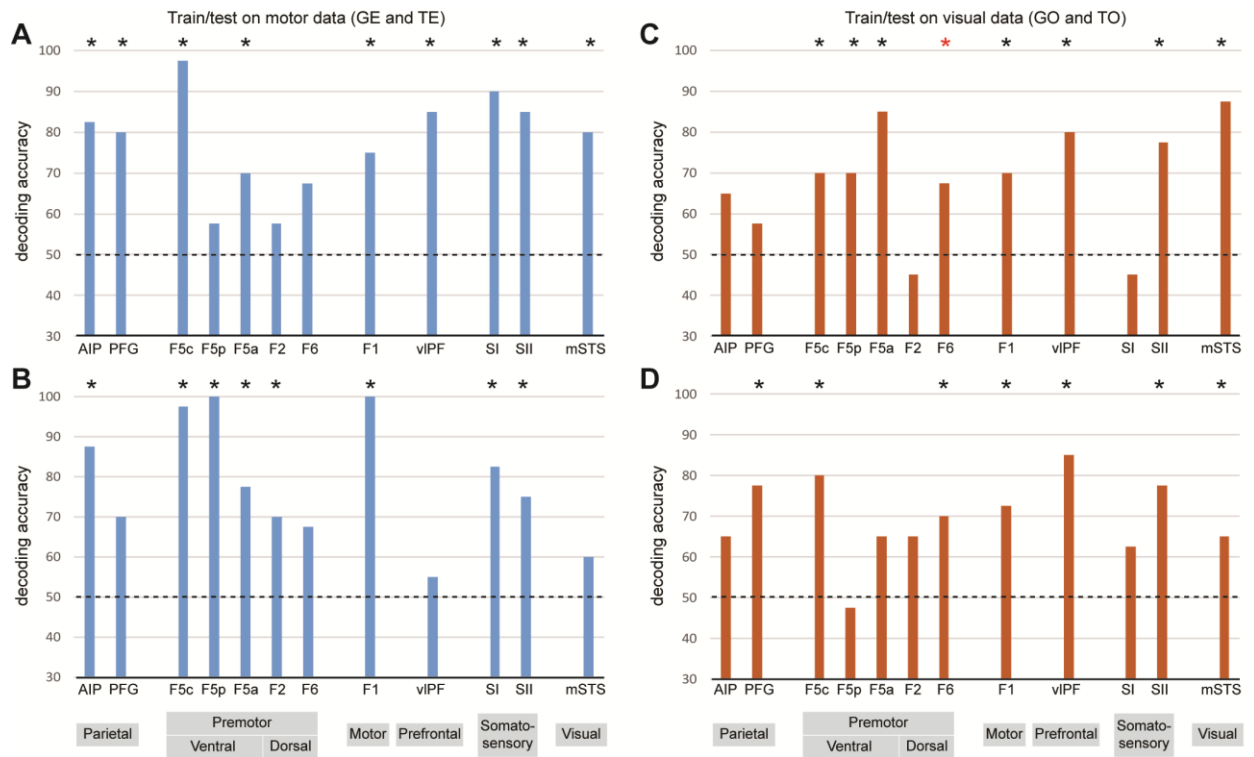
Figure 3. Unimodal decoding of executed or observed actions.

A,B. Unimodal decoding of executed actions with the right hand in contralateral (left) hemisphere of monkeys M1 (A) and M2 (B): executed reach-and-grasp (GE) or reach-and-touch (TE) motor acts could be decoded significantly above chance ($p < 0.05$, corr.) from parietal areas AIP and PFG, ventral premotor areas F5c and F5a, dorsal premotor areas F2 and F6, primary motor area F1, secondary (SII) somatosensory cortex and ventrolateral prefrontal cortex (vlPF) in monkey M1 and from parietal areas AIP and PFG, ventral premotor areas F5c, F5p and F5a, dorsal premotor areas F2, primary motor area F1, primary (SI) and secondary (SII) somatosensory cortex and ventrolateral prefrontal cortex (vlPF) in monkey M2. Black asterisks indicate significance level ($p < 0.05$, corr.).

C,D. Unimodal decoding of observed actions in left hemisphere of monkeys M1 (C) and M2 (D): observed reach-and-grasp (GO) or reach-and-touch (TO) actions yielded significantly ($p < 0.05$, corr.) different voxel patterns in parietal areas AIP and PFG, ventral premotor areas F5c and F5a, secondary (SII) somatosensory cortex, ventrolateral prefrontal cortex (vlPF) and STS (mSTS) in monkey M1 (C) and in parietal areas AIP and PFG, ventral premotor areas F5c, F5p and F5a, primary motor cortex F1, secondary (SII) somatosensory cortex, ventrolateral prefrontal cortex (vlPF) and STS (mSTS) in monkey M2 (D). Black asterisks indicate significance level ($p < 0.05$, corr.).

Supplementary Figure 4. Unimodal decoding of executed or observed actions in ipsilateral hemisphere.

A,B. Unimodal decoding of executed actions with the right hand in ipsilateral (right) hemisphere of monkeys M1 (A) and M2 (B): executed reach-and-grasp (GE) or reach-and-touch (TE) motor acts could be decoded significantly above chance (p < 0.05, corr.) from parietal areas AIP and PFG, ventral premotor areas F5c and F5a, primary motor area F1, primary (SI) and secondary (SII) somatosensory cortices, ventrolateral prefrontal cortex (vlPF) and mSTS in monkey M1 and from parietal area AIP, ventral premotor areas F5c, F5p and F5a, dorsal premotor areas F2, primary motor area F1, primary (SI) and secondary (SII) somatosensory cortices in monkey M2. Black asterisks indicate significance level (p < 0.05, corr.).

C,D. Unimodal decoding of observed actions in right hemisphere of monkeys M1 (C) and M2 (D): observed reach-and-grasp (GO) or reach-and-touch (TO) actions yielded significantly (p < 0.05, corr.) different voxel patterns in ventral premotor areas F5c, F5p and F5a, primary motor area F1, secondary (SII) somatosensory cortex, ventrolateral prefrontal cortex (vlPF) and mSTS in monkey M1 (C) and in parietal area PFG, ventral premotor area F5c, dorsal premotor area F6, primary motor cortex F1, secondary (SII) somatosensory cortex, ventrolateral prefrontal cortex (vlPF) and mSTS in monkey M2 (D). Black and red asterisks indicate significance level (respectively p < 0.05, corr. and p < 0.05, uncorr.).

23

Based on the claim that mirror neurons underlie action simulation and map observed actions onto their corresponding motor representation (Rizzolatti and Sinigaglia, 2016), one would expect to find more similar voxel representations for the same actions compared to different actions, across visual and motor modalities (Oosterhof et al., 2013). To assess this we performed two cross-modal decoding tests, by either using the visual data as the input for training the classifiers and the corresponding motor data for testing (Fig.4A,B; Suppl. Fig.5A,B), or vice-versa (Fig.4C,D; Suppl.Fig.5C,D). In the contralateral (left) hemisphere, we found significant ($p < 0.05$, corr.) cross-modal action-specific decoding in both subjects in parietal areas AIP and PFG, ventral premotor F5c, primary motor area F1, and SII (Fig.4A,B). In addition significant cross-modal decoding was found in F5a in monkey M1 and in F5a and vlPF in monkey M2. This effect however, was largely asymmetrical, only present when classifiers were trained with the data from the visual modality and tested on the data from the motor modality (Fig.4A,B). Training with motor data and testing on visual data only yielded above chance decoding in AIP in monkey M1 (Fig.4C) and in vlPF in monkey M2, at $p < 0.05$, uncorr. Investigation of the ROIs in ipsilateral right hemisphere only yielded significant ($p < 0.05$, corr.) cross-modal action-specific decoding in both subjects in somatosensory SII and premotor F2 for monkey M2 when classifiers were trained with the data from the visual modality and tested on the data from the motor modality (Suppl. Fig.5A,B). Similar to the contralateral hemisphere, training and testing in the other direction (motor to visual), did not yield significant classification (after correction) in any of the ROIs tested in the ipsilateral hemisphere (Suppl. Fig.5C,D) (only SI in monkey M2 reached $p < 0.05$, uncorr.).
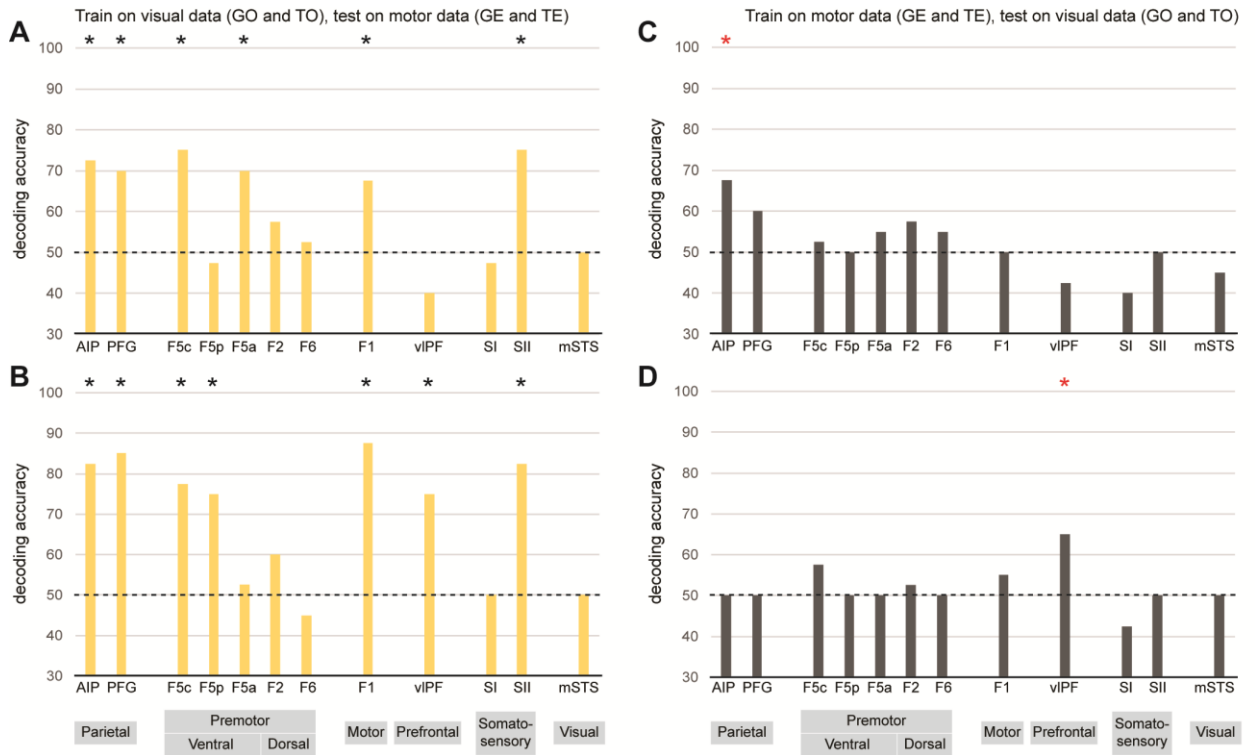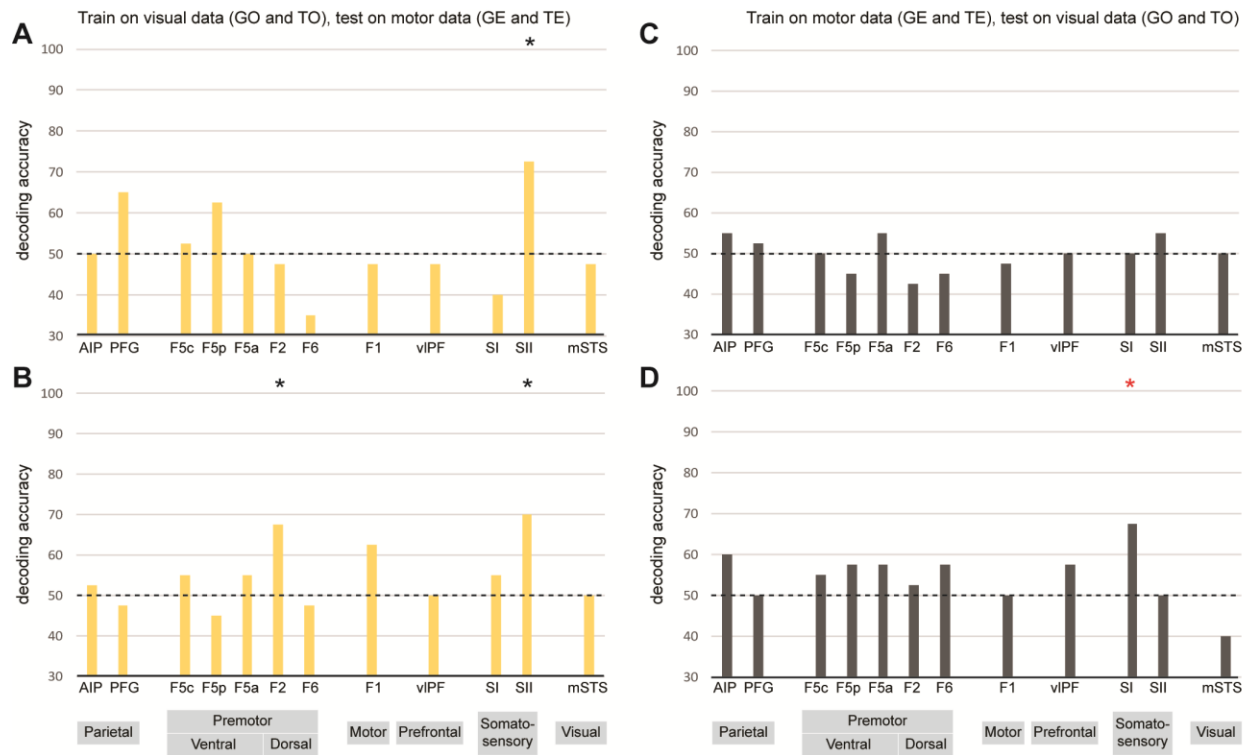
Figure 4. Cross-modal decoding of executed and observed actions.

A,B. Classifiers trained with visual data (reach-and-grasp and reach-and-touch observation) and tested with motor data (reach-and-grasp and reach-and-touch execution) showed significant ($p < 0.05$, corr., black asterisks) cross-modal action-specific decoding in both subjects in parietal areas AIP and PFG, ventral premotor F5c, F1, and SII. In addition, in monkey M1 (A), significant cross-modal action-specific decoding was also found in F5a, and in F5p and vlPF in monkey M2 (B).

C,D. Classifiers trained with motor data (reach-and-grasp and reach-and-touch execution) and tested with visual data (reach-and-grasp and reach-and-touch observation) did not yield significant (at $p < 0.05$, corr.) decoding accuracies in any of the ROIs tested. At $p < 0.05$, uncorr. (red asterisks), only AIP in monkey M1 (C) and vlPF in monkey M2 (D) yielded significant cross-modal decoding.

Supplementary Figure 5. Cross-modal decoding of executed and observed actions in ipsilateral hemisphere.

A,B. Classifiers trained with visual data (reach-and-grasp and reach-and-touch observation) and tested with motor data (reach-and-grasp and reach-and-touch execution) showed significant ($p < 0.05$, corr., black asterisks) cross-modal action-specific decoding in both subjects in somatosensory SII (A,B). In addition, in monkey M2, significant cross-modal action-specific decoding was also found in dorsal premotor F2 (B).

C,D. Classifiers trained with motor data (reach-and-grasp and reach-and-touch execution) and tested with visual data (reach-and-grasp and reach-and-touch observation) did not yield significant (at $p < 0.05$, corr.) decoding accuracies in any of the ROIs tested. At $p < 0.05$, uncorr. (red asterisk), only SI in monkey M2 (D) significant cross-modal decoding.

Discussion

Here, for the first time, we used cross-modal fMRI classification as a method to probe common coding of observed and executed actions in non-human primates. Rhesus monkeys were trained to either perform two different motor actions with their right hand (without visual feedback) or observe videos of humans performing similar actions. We specifically analyzed the

patterns of activity across voxels in brain regions known to play a role in action execution and/or observation. The key observations of our study are: 1) brain regions known to house mirror neurons including rostral parietal, premotor and motor regions, showed significant cross-modal action-specific decoding in monkeys; 2) additional regions tightly linked to the grasping motor network such as secondary somatosensory cortices also yielded similar shared representations between observed and executed actions; 3) the cross-modal classification results were mostly asymmetrical, yielding significant cross-modal decoding when training classifiers with visual data and testing with motor data, but not when training with motor data and testing with visual data; 4) a portion of monkey STS, possibly homologous to part of human OT, did not show any cross-modal action-specific effects.

Comparison of monkey cross-modal fMRI classification with electrophysiology data on mirror neurons

The majority of mirror neuron studies in monkeys have investigated ventral premotor area F5c, or area PFG located in the rostral part of the inferior parietal lobule (IPL). Our fMRI decoding study shows that both regions, in addition to allowing unimodal decoding for both executed and observed actions, also yield significant cross-modal classification (especially when training classifiers on observation data and testing on execution data). These results suggest that cross-modal fMRI classification is indeed able to retrieve shared representations of own and others' actions, possibly mediated by mirror neurons in these regions (Etzel et al., 2008; Oosterhof et al., 2013). Our current findings fits well with respect to the proposed functional specialization suggested for premotor area F5. Based upon cytoarchitectonic, connectional and functional data, it has been shown that F5 consists of 3 subparts: F5c on the convexity posterior to the inferior ramus of the arcuate sulcus (IAS), F5p in the posterior portion of the posterior bank of the IAS and F5a in the more anterior deeper portion of the posterior bank of the IAS (Rizzolatti and Luppino, 2001; Nelissen et al., 2005; Belmalih et al., 2009; Gerbella et al., 2011). Previous univariate fMRI investigations in monkeys have shown that all three F5 sectors (F5c, F5p and F5a) show grasping-related motor responses (Nelissen and Vanduffel, 2011), in addition to action observation responses (Nelissen et al., 2005). Our current MVPA study suggests that although unimodal decoding of motor and visual actions was possible in most of the F5

subregions (except for F5p in monkey M1), shared representations between executed and observed actions are particularly evident in voxel patterns from F5c in both subjects, where mirror neurons are primarily found (for review see Kilner and Lemon, 2013, Rozzi and Coudé, 2015; Bonini, 2016).

While the mirror neuron system in monkeys is often still thought of as consisting of 2 regions (parietal PFG and premotor F5c), more recent investigations from several groups have shown that mirror neurons or mirror-like activity is also found in many additional brain regions (for review see Kilner and Lemon, 2013), including parietal area AIP (Pani et al., 2014), primary motor cortex F1 or M1 (Dushanova and Donoghue, 2010; Tkach et., 2007; Vigneswaran et al., 2013), frontal and prefrontal cortex (Cisek and Kalaka, 2004; Yoshida et al., 2011; Falcone et al., 2016; Simone et al., 2017). Our results showing shared responses between observed and executed actions in areas AIP and F1 support these previous single cell reports (Dushanova and Donoghue, 2010; Tkach et., 2007; Vigneswaran et al., 2013; Pani et al., 2014). Since previous electrophysiology data from humans (Mukamel et al., 2010) and monkeys (Cisek and Kalaska, 2004; Yoshida et al., 2011) have shown mirror-like activity in dorsal premotor cortices when either performing actions or monitoring others' actions, we also investigated area F2 and pre-supplementary motor area (pre-SMA) F6 in the current study. Our results found little empirical support for shared representations in these regions at the voxel level, at least for the two actions used in our study. Currently it is not clear to what extent the different subparts of dorsal premotor cortices in the monkeys contain mirror neurons and if such neurons would possess similar or different visuo-motor properties as the mirror neurons typically described in ventral premotor and parietal cortices. Given its previously established roles in updating of motor plans (Shima et al., 1996), performance monitoring (Scangos et al., 2013) and organizing complex motor sequences (Tanji, 2001), it might be that shared responses in pre-SMA become more evident during more complex action execution and observation tasks than the one used in our current study, possibly involving competitive or cooperative tasks during which monkeys have to perform or observe actions in a social context (Yoshida et al., 2011). Future electrophysiology and monkey fMRI experiments investigating action observation and execution in similar social settings will be needed to answer these open questions (Rozzi and Coudé, 2015; Bonini, 2016).

Recently it was suggested that a portion of the ventrolateral prefrontal cortex (vlPF), including area 46v, might also be part of the broader mirror neuron network (Bonini, 2016). The

role of monkey prefrontal cortex in different aspects of goal and action planning and selection has long been established (Hoshi et al., 2000; Saito et al., 2005; Averbeck et al., 2006). More recently, it was shown that this sector of the brain contains neurons specifically responding during the execution of goal-directed grasping actions performed with or without visual feedback (Simone et al., 2015; Bruni et al., 2015; Raos and Savaki, 2016b). This response profile is similar to grasping-related neurons found in parietal and premotor cortices. In addition, anatomical data shows that this region is closely linked to the brain network controlling goal-directed actions (Borra et al., 2011; Gerbella et al., 2013). A recent single cell study investigating action observation in vlPF showed that a small fraction of the recorded neurons could be classified as mirror neurons based upon their response profile (Simone et al., 2017). In line with its role in action generation and perception (Simone et al., 2015; Bruni et al., 2015; Raos and Savaki, 2016b) and the demonstration of grasping-related mirror neurons (Simon et al., 2017) in this region, Falcone and co-authors (2016) recently showed that ventrolateral prefrontal cortex contains neurons that encode both own and others' future goals. Although we only found cross-modal shared representations between observed and executed actions in this region in one out of the two subjects, this finding seems to be in agreement with former mentioned electrophysiological and imaging observations. Additional investigations are needed to determine the possible extent of mirror neurons and their exact functional characteristics throughout the prefrontal cortex.

In this cross-modal MVPA study we focused our analysis on regions-of-interest that were previously shown to contain mirror neurons, and a few additional candidate regions that have been linked to the mirror neuron system based on either preliminary electrophysiology examinations or anatomical and functional links with the motor system. It is possible however that other regions not examined here might also yield similar shared representations between executed and observed actions. Future studies of non-human primates should investigate shared representations of actions combining whole-brain approaches, for example search-light MVPA (Kriegeskorte et al., 2006; Oosterhof et al., 2010), followed by single-cell recordings to address critical questions such as 1) how extended these shared representations in the monkey brain are, and 2) if regions that show cross-modal action-specific responses at the voxel level also show multimodal action responses at the single neuron level.

Cross-modal multi-variate fMRI classification as a tool to investigate shared representations of own and others' actions in the brain

At present, the limited number of studies using cross-modal MVPA to study common coding of own and others' actions in the human brain have produced mixed results (for review see Oosterhof et al., 2013; Kaplan et al., 2015). Some of these inconsistencies might be related to the different tasks used in these studies and the different analytical approaches. The first study to test the simulation theory of actions by employing cross-modal MVPA (Etzel et al., 2008), trained classifiers with auditory data (sounds associated with either transitive hand or mouth actions) and tested on the corresponding motor data (execution of transitive hand or mouth actions). From all anatomical ROIs examined in that study, only bilateral premotor cortex allowed significant cross-modal classification, although the authors also reported that a functionally defined ROI in the right parietal cortex also yielded significant cross-modal decoding. In the same year, Dinstein and colleagues (2008) investigated unimodal and cross-modal decoding using intransitive actions (execution or observation of rock, paper and scissors hand gestures). They reported that albeit anterior intraparietal sulcus (aIPS) showed significant unimodal classification for both executed and observed hand gestures, this region failed to show cross-modal decoding greater than chance. Oosterhof et al. (2010) on the other hand, examined cross-modal decoding of actions throughout the whole human brain using search-light MVPA and surface-based analysis approaches. These authors found significant cross-modal decoding for both intransitive and transitive actions in a region that included the contralateral anterior parietal cortex in addition to a portion of somatosensory cortices, as well as bilateral occipito-temporal (OT) cortex. While this initial study failed to show shared representations of executed and observed actions in human premotor cortex, in a later study Oosterhof and co-workers (2012b) showed cross-modal classification in left premotor cortex, when subjects observed actions from a first-person but not from a third-person perspective. This led the authors to suggest action representations in premotor cortex might be view-dependent, as opposed to those in parietal and potentially OT cortices. Our current findings in the monkey show a similar bias of cross-modal action-specific decoding towards the contralateral hemisphere as previously observed in these human MVPA studies (Oosterhof et al., 2010, 2012b). While our current study does not allow to draw inferences about viewpoint-dependency of action representations in

monkeys (de la Rosa et al., 2013; Platonov and Orban, 2016), we did find cross-modal action-specific action representations when the subjects observed actions from a third-person perspective. This is in line with numerous electrophysiology studies of mirror neurons in F5, most of which have investigated mirror neurons by having monkeys observe actions from a third-person perspective (Gallese et al., 1996; Kilner and Lemon, 2013; Bonini, 2016).

Both humans (Allison et al., 2000; Oosterhof et al, 2013; Wurm and Lingnau, 2015; Vander Wyk et al., 2012; Deen et al., 2015; Jastorff et al., 2016) and monkeys (Perrett et al., 1989; Puce and Perrett, 2003; Barraclough et al., 2009; Nelissen et al., 2006, 2011; Jastorff et al., 2012) have several regions in extrastriate visual cortex that have been shown to play a particular role in action recognition. As mentioned earlier, some human MVPA studies investigating common coding of actions have reported cross-modal action-specific effects in the lateral occipito-temporal (OT) cortex (Oosterhof et al., 2010, Oosterhof et al., 2012a). The large OT cluster identified in those studies is suggested (Oosterhof et al., 2010) to include several functional regions like MT complex (Tootell et al., 1995; Huk et al., 2002) and EBA (Downing et al., 2001; Astafiev et al., 2004), in addition to portions of the lateral occipital complex (LOC). While in our study the monkey functional homologue of this human OT cluster did yield significant decoding for unimodal observed actions, it failed to show cross-modal action-specific representations. This finding suggests that, although monkey STS should be regarded as an important stage for the visual analysis of body movements and actions (Perrett et al., 1989; Puce and Perrett, 2003; Barraclough et al., 2009; Nelissen et al., 2006, 2011; Jastorff et al., 2012; Giese and Rizzolatti, 2015), it does not seem to share the same functional characteristics as the parieto-frontal mirror neuron regions (Rizzolatti et al., 2001). To date, single cell data is yet to demonstrate the presence of neurons with motor properties in monkey STS, similar to those found in grasping-related parietal and premotor regions. Future functional imaging studies comparing humans with monkeys (Mantini et al., 2012; Caspari et al., 2017) will be useful in establishing more detailed species commonalities and/or differences of this portion of the cortex in representing own and others' actions in both humans and monkeys.

Asymmetries in cross-modal multi-voxel fMRI classifications

Our cross-modal action decoding analyses showed a clear asymmetry: for most regions cross-modal classification was only possible when using the visual data as training input for the classifiers and testing on motor data. So far, the directional effects of cross-modal classification results are not fully understood (Kaplan et al., 2015). The previous studies that have used cross-modal classification for investigating common coding for actions in humans have taken different approaches related to directionality. Some have chosen to average results from both directions (Oosterhof et al., 2010, 2012a), whereas others report both directions separately (Dinstein et al., 2008, Oosterhof et al., 2012b; Zabicki et al., 2016) or only report one direction (Etzel et al., 2008).

It is often assumed that these cross-modal action-specific effects should yield symmetrical (Grigaityte and Iacoboni, 2015; Oosterhof et al., 2010, 2012a) results irrespective of direction (i.e. from visual to motor and vice-versa). However, this assumption overlooks the essential heterogeneous response characteristics of neurons found in motor regions and the fact that mirror neurons are only a small fraction of the neurons found in these regions. Therefore, relatively strong (or, at least, less noisy) patterns learned from training with motor task data from mirror neuron regions (during which a large fraction of motor neurons become active) do not necessarily transfer to weaker (more noisy) patterns present in the visual task data (when only a small fraction of neurons become activated) obtained from these regions. This is the reason that Etzel and co-workers (2008) only reported cross-modal decoding results from one direction (training with auditory data, testing with motor data).

Interestingly, recent human studies investigating the similarities in multi-voxel patterns during execution or imagery of actions also seem to suggest a similar asymmetry. Although subtle, data from Zabicki et al. (2016) showed that classifiers yielded more significant decoding results when trained on data from imagined actions and tested on data from executed actions than vice-versa. Another human MVPA study comparing imagined actions with executed actions (Oosterhof et al., 2012b) directly tested for symmetry in their decoding results. Oosterhof and co-workers reported better classifier performance when training on imagined trials and testing on performed trials than vice-versa, which according to the authors might be explained in terms of the strength of the pattern information used to train the classifiers. Since in our current experiment monkeys only performed one particular reach-and-grasping movement (always grasping the same object), while they observed different examples of reach-and-grasp

movements in the observation condition, it is difficult the make conclusive statements about the potential source of the asymmetry in our data in terms of richness or sparseness of information in the voxel patterns when observing or executing a particular action. While future experiments specifically designed to examine the source of these asymmetries will be needed (Kaplan et al., 2015), in view of previous asymmetric cross-modal decoding results in humans, our data suggest that averaging results from cross-modal tests in both directions (Oosterhof et al., 2010, 2012a) could potentially lead to false negative results and therefore it seems better to report cross-modal results in both directions separately (Kaplan et al., 2015; Oosterhof et al., 2012b; Zabicki et al., 2016).

Shared representations for observed and executed actions in monkey somatosensory cortices?

An apparent discrepancy that have emerged in recent years from studies investigating shared responses in the human and non-human primate brain, relates in particular to the somatosensory cortices. While a number of studies have suggested vicarious responses in human primary and/or secondary somatosensory cortices during either specific instances of touch observation or more in general action observation (Keysers et al., 2004; Blakemore et al., 2005; Pihko et al., 2010; Meyer et al., 2011; for a review see Keysers et al., 2010), other human fMRI investigations found little evidence for touch observation related responses in somatosensory cortices (Chan and Baker, 2015). Although detailed single cell investigations with respect to the possible presence of mirror neurons, or shared responses for observed and executed actions, in monkey SI and SII have not yet been performed, data from neuroimaging together with electrophysiology studies have suggested that monkey somatosensory cortices respond during both action observation and execution (Evangeliou et al., 2009; Raos et al., 2004, 2007; Nelissen and Vanduffel, 2011; Ishida et al., 2013; Hihara et al., 2015; Raos and Savaki, 2016a). Recently, Sharma and co-authors found univariate fMRI responses during both grasping execution and grasp or touch observation in a portion of monkey SII cortex (Sharma et al., 2018). In line with human cross-modal MVPA studies that have found shared responses during action observation and execution in somatosensory cortices (Oosterhof et al., 2010, 2013), our current data suggest similar shared representations of own and others' actions might also be present in somatosensory cortices of the monkey, at least in SII. Additional investigations will be needed to examine the

extent and the exact characteristics of these shared responses in monkey somatosensory cortices and their underlying neuronal source.

In conclusion, our results support the promising application of multi-variate approaches in studying the neural correlates of simulation or common coding theories of action. Our findings are in line with the claim that, besides the visual and STS cortices (Barraclough et al., 2009; Nelissen et al., 2011; Jastorff et al., 2012; Giese and Rizzolatti, 2015; Lingnau and Downing, 2015), also individuals' own motor system, and possibly somatosensory cortices, are involved in representing others' actions (Keysers et al., 2010; Rizzolatti and Sinigaglia, 2016). Future studies employing parallel multi-variate investigations in both human and non-human primates will be pivotal in unravelling the similarities and differences of shared representations of actions across species. An important question that still needs to be answered is to what extent these shared actions representations in the primate brain underlie different cognitive and/or social functions.

References

Allison T, Puce A, McCarthy G. 2000. Social perception from visual cues: role of the STS region.
Trends Cogn Sci. 4: 267-278.

Astafiev SV, Stanley CM, Shulman GL, Corbetta M. 2004. Extrastriate body area in human occipital cortex responds to the performance of motor actions. Nat Neurosci. 7: 542-8.

Averbeck BB, Sohn JW, Lee D. 2006. Activity in prefrontal cortex during dynamic selection of action sequences. Nat Neurosci. 9: 276-82.

Barraclough NE, Keith RH, Xiao D, Oram MW, Perrett DI. 2009. Visual adaptation to goal-directed hand actions. J Cogn Neurosci. 21: 1806-20.

Belmalih A, Borra E, Contini M, Gerbella M, Rozzi S, Luppino G. 2009. Multimodal architectonic subdivision of the rostral part (area F5) of the macaque ventral premotor cortex. J Comp Neurol. 512:183-217.

Blakemore SJ, Bristow D, Bird G, Frith C, Ward J (2005) Somatosensory activations during the observation of touch and a case of vision-touch synaesthesia. Brain 128:1571–1583.

Bonini L. 2016. The extended mirror neuron network: anatomy, origin, and functions. Neuroscientist 23: 56–67.

Bonini L, Ugolotti Serventi F, Bruni S, Maranesi M, Bimbi M, Simone L, Rozzi S, Ferrari PF, Fogassi L. 2012. Selectivity for grip type and action goal in macaque inferior parietal and ventral premotor grasping neurons. J Neurophysiol. 108: 1607–1619.

Borra E, Gerbella M, Rozzi S, Luppino G. 2011. Anatomical evidence for the involvement of the macaque ventrolateral prefrontal area 12r in controlling goal-directed actions. J Neurosci. 31:12351-63.

Borra E, Gerbella M, Rozzi S, Luppino G. 2017. The macaque lateral grasping network: a neural substrate for generating purposeful hand actions. Neurosci Biobehav Rev. 75: 65-90.

Bruni S, Giorgetti V, Bonini L, Fogassi L. 2015. Processing and Integration of Contextual Information in Monkey Ventrolateral Prefrontal Neurons during Selection and Execution of Goal-Directed Manipulative Actions. J Neurosci. 35: 11877-90.

Caspari N, Arsenault JT, Vandenberghe R, Vanduffel W. 2017. Functional Similarity of Medial Superior Parietal Areas for Shift-Selective Attention Signals in Humans and Monkeys. Cereb Cortex. 4: 1-15.

Caspari N, Popivanov ID, De Mazière PA, Vanduffel W, Vogels R, Orban GA, Jastorff J. 2014. Fine-grained stimulus representations in body selective areas of human occipito-temporal cortex. Neuroimage. 102: 484-97.

Caspers S, Zilles K, Laird AR, Eickhoff SB. 2010. ALE meta-analysis of action observation and imitation in the human brain. Neuroimage. 50:1148-67.

Chan AW, Baker CI (2015) Seeing Is Not Feeling: Posterior Parietal But Not Somatosensory Cortex Engagement During Touch Observation. J Neurosci 35:1468–1480.

Chong TT, Cunnington R, Williams MA, Kanwisher N, Mattingley JB. 2008. fMRI adaptation reveals mirror neurons in human inferior parietal cortex. Curr Biol. 18: 1576-80.

Cisek P, Kalaska JF. 2004. Neural correlates of mental rehearsal in dorsal premotor cortex. Nature. 431: 993-6.

Cook R, Bird G, Catmur C, Press C, Heyes C. 2014. Mirror neurons: from origin to function. Behav Brain Sci. 37: 177-92.

Deen B, Koldewyn K, Kanwisher N, Saxe R. 2015. Functional Organization of Social Perception and Cognition in the Superior Temporal Sulcus. Cereb Cortex. 25: 4596-609.

de la Rosa, S., Mieskes, S., Bülthoff, H.H. & Curio, C. View dependencies in the visual recognition of social interactions. Front Psychol. 4: 752.

de la Rosa S, Schillinger FL, Bülthoff HH, Schultz J, Uludag K. 2016. fMRI Adaptation between Action Observation and Action Execution Reveals Cortical Areas with Mirror Neuron Properties in Human BA 44/45. Front Hum Neurosci. 10:78.

Dinstein I, Gardner JL, Jazayeri M, Heeger DJ. 2008. Executed and observed movements have different distributed representations in human aIPS. J Neurosci. 28: 11231-11239.

di Pellegrino G, Fadiga L, Fogassi L, Gallese V, Rizzolatti G. 1992. Understanding motor events: a neurophysiological study. Exp Brain Res. **91**, 176–180.

Downing PE, Jiang Y, Shuman M, Kanwisher N. 2001. A cortical area selective for visual processing of the human body.Science. 293: 2470-3.

Durand JB, Nelissen K, Joly O, Wardak C, Todd JT, Norman JF, Janssen P, Vanduffel W, Orban GA. 2007. Anterior regions of monkey parietal cortex process visual 3D shape. Neuron. 55:493-505.

Dushanova J, Donoghue J. Neurons in primary motor cortex engaged during action observation. Eur J Neurosci. 31: 386-398.

Ebisch SJ, Perrucci MG, Ferretti A, Del Gratta C, Romani GL, Gallese V. 2008. The sense of touch: embodied simulation in a visuotactile mirroring mechanism for observed animate or inanimate touch. J Cogn Neurosci. 20: 1611-1623.

Ekstrom LB, Roelfsema PR, Arsenault JT, Bonmassar G, Vanduffel W. 2008. Bottom-up dependent gating of frontal signals in early visual cortex. Science. 321:414-417.

Etzel JA, Gazzola V, Keysers C. 2008. Testing simulation theory with cross-modal multi-variate classification of fMRI data. PLoS One. 3: e3690.

Evangeliou MN, Raos V, Galletti C, Savaki HE. 2009. Functional imaging of the parietal cortex during action execution and observation. Cereb Cortex. 19: 624-39.

Falcone R, Brunamonti E, Ferraina S, Genovesio A. 2016. Neural Encoding of Self and Another Agent's Goal in the Primate Prefrontal Cortex: Human-Monkey Interactions. Cereb Cortex. 26 :4613-4622.

Ferrari PF, Rozzi S, Fogassi L. 2005. Mirror neurons responding to observation of actions made with tools in monkey ventral premotor cortex. J Cogn Neurosci. 17: 212-226.

Fogassi L, Ferrari PF, Gesierich B, Rozzi S, Chersi F, Rizzolatti G. 2005. Parietal lobe: from action organization to intention understanding. Science. 308: 662-667.

Friston KJ, Holmes AP, Worsley KJ, Poline JB, Frackowiak RSJ. 1995. Statistical parametric maps in functional imaging: a general approach. Hum Brain Mapp. 2:189-210.

Gallese V, Fadiga L, Fogassi L, Rizzolatti G. 1996. Action recognition in the premotor cortex. Brain. 119: 593-609.

Gerbella M, Belmalih A, Borra E, Rozzi S, Luppino G. 2011. Cortical connections of the anterior (F5a) subdivision of the macaque ventral premotor area F5. Brain Struct Funct. 216: 43-65.

Gerbella M, Borra E, Tonelli S, Rozzi S, Luppino G. 2013. Connectional heterogeneity of the ventral part of the macaque area 46. Cereb Cortex 23: 967-987.

Giese MA, Rizzolatti G. 2015. Neural and computational mechanisms of action processing: interaction between visual and motor representations. Neuron. 88: 167–180.

Grafton ST. 2010. The cognitive neuroscience of prehension: recent developments. Exp Brain Res. 204:475-491.

Gregoriou GG, Borra E, Matelli M, Luppino G. 2006. Architectonic organization of the inferior parietal convexity of the macaque monkey. J Comp Neurol. 496:422-451.

Grigaityte K, Iacoboni M. 2015. Chapter 5, In: New Frontiers in mirror neuron research. Editors: P.F. Ferrari, G. Rizzolatti, Oxford Press.

Grill-Spector K, Malach R. 2001. fMR-adaptation: a tool for studying the functional properties of human cortical neurons. Acta Psychol (Amst). 107: 293-321.

Haxby JV, Gobbini MI, Furey ML, Ishai A, Schouten JL, Pietrini P. 2001. Distributed and overlapping representations of faces and objects in ventral temporal cortex. Science. 293: 2425-30.

Hebart MN, Görgen K, Haynes JD. 2015. The Decoding Toolbox (TDT): a versatile software package for multi-variate analyses of functional imaging data. Front Neuroinform. 8:88.

Hickok G. 2013. Do mirror neurons subserve action understanding? Neurosci Lett. 540:56-8.

Hihara S, Taoka M, Tanaka M, Iriki A. 2015. Visual Responsiveness of Neurons in the Secondary Somatosensory Area and its Surrounding Parietal Operculum Regions in Awake Macaque Monkeys. Cereb Cortex. 25: 4535-50.

Hoshi E, Shima K, Tanji J.2000. Neuronal activity in the primate prefrontal cortex in the process of motor selection based on two behavioral rules. J Neurophysiol. 83: 2355-73.

Huk AC, Dougherty RF, Heeger DJ. 2002. Retinotopy and functional subdivision of human areas MT and MST. J Neurosci. 22: 7195-205.

Ishida H, Fornia L, Grandi LC, Umiltà MA, Gallese V. 2013. Somato-motor haptic processing in posterior inner perisylvian region (SII/pIC) of the macaque monkey. PLoS One. 8: e69931.

Jastorff J, Popivanov ID, Vogels R, Vanduffel W, Orban GA. 2012. Integration of shape and motion cues in biological motion processing in the monkey STS. Neuroimage. 60: 911-21.

Jastorff J, Abdollahi RO, Fasano F, Orban GA. 2016. Seeing biological actions in 3D: An fMRI study. Hum Brain Mapp. 37: 203-19.

Jeannerod M. 2001. Neural simulation of action: a unifying mechanism for motor cognition. NeuroImage. 14: S103–S109.

Kaplan JT, Man K, Greening SG. 2015. Multi-variate cross-classification: applying machine-learning techniques to characterize abstraction in neural representations. Front Hum Neurosci. 9: 151.

Keysers C, Gazzola V. 2009. Expanding the mirror: vicarious activity for actions, emotions, and sensations. Curr Opin Neurobiol. 19: 666-671.

Keysers C, Kaas JH, Gazzola V. 2010. Somatosensation in social perception. Nat Rev Neurosci 11:417–428.

Keysers C, Wicker B, Gazzola V, Anton JL, Fogassi L, Gallese V. 2004. A touching sight: SII/PV activation during the observation and experience of touch. Neuron. 42: 335-46.

Kilner JM, Neal A, Weiskopf N, Friston KJ, Frith CD. 2009. Evidence of mirror neurons in human inferior frontal gyrus. J Neurosci. 29: 10153-9.

Kilner JM, Lemon RN. 2013. What we know currently about mirror neurons. Curr Biol 23: R1057–R1062.

Kolster H, Mandeville JB, Arsenault JT, Ekstrom LB, Wald LL, Vanduffel W. 2009. Visual field map clusters in macaque extrastriate visual cortex. J Neurosci. 29:7031-7039.

Kriegeskorte N, Goebel R, Bandettini P. 2006. Information-based functional brain mapping. Proc Natl Acad Sci U S A. 103: 3863-8.

Lingnau A, Gesierich B, Caramazza A. 2009. Asymmetric fMRI adaptation reveals no evidence for mirror neurons in humans. Proc Natl Acad Sci USA. 106: 9925-9930.

Mandeville JB, Marota JJ. 1999. Vascular filters of functional MRI: spatial localization using BOLD and CBV contrast. Magn Reson Med. 42: 591-598.

Mantini D, Hasson U, Betti V, Perrucci MG, Romani GL, Corbetta M, Orban GA, Vanduffel W. 2012. Interspecies activity correlations reveal functional correspondence between monkey and human brain areas. Nat Methods. 9: 277-82.

Maranesi M, Rodà F, Bonini L, Rozzi S, Ferrari PF, Fogassi L, Coudé G. 2012. Anatomo-functional organization of the ventral primary motor and premotor cortex in the macaque monkey. Eur J Neurosci. 36: 3376-87.

Meyer K, Kaplan JT, Essex R, Damasio H, Damasio A (2011) Seeing Touch Is Correlated with Content-Specific Activity in Primary Somatosensory Cortex. Cereb Cortex 21:2113–2121.

Molenberghs P, Cunnington R, Mattingley JB. 2012. Brain regions with mirror properties: a meta-analysis of 125 human fMRI studies. Neurosci Biobehav Rev. 36:341-9.

Mooney R. 2014. Auditory–vocal mirroring in songbirds. Philos Trans R Soc Lond B Biol Sci. 369: 20130179.

Mukamel R, Ekstrom AD, Kaplan J, Iacoboni M, Fried I. 2010. Single-neuron responses in humans during execution and observation of actions. Curr Biol. 20: 750-6.

Murata A, Gallese V, Luppino G, Kaseda M, Sakata H. 2000. Selectivity for the shape, size, and orientation of objects for grasping in neurons of monkey parietal area AIP. J Neurophysiol. 83: 2580–2601.

Nelissen K, Borra E, Gerbella M, Rozzi S, Luppino G, Vanduffel W, Rizzolatti G, Orban GA. 2011. Action observation circuits in the macaque monkey cortex. J Neurosci. 31: 3743-3756.

Nelissen K, Fiave PA, Vanduffel W. 2017. Decoding grasping movements from the parieto-frontal reaching circuit in the nonhuman primate. Cereb Cortex. *Epub ahead of print*.

Nelissen K, Luppino G, Vanduffel W, Rizzolatti G, Orban G. 2005. Observing others: Multiple action representation in the frontal lobe. Science. 310: 332-336.

Nelissen K, Vanduffel W. 2011. Grasping-related functional magnetic resonance imaging brain responses in the macaque monkey. J Neurosci 26: 5929-5947.

Nelissen K, Vanduffel W, Orban GA. 2006. Charting the lower superior temporal region, a new motion-sensitive region in monkey superior temporal sulcus. J Neurosci. 26: 5929-5947.

Norman KA, Polyn SM, Detre GJ, Haxby JV. 2006. Beyond mind-reading: multi-voxel pattern analysis of fMRI data. Trends Cogn Sci. 10: 424-430.

Oosterhof NN, Tipper SP, Downing PE. 2013. Cross-modal and action-specific: neuroimaging the human mirror neuron system. Trends Cogn Sci. 17: 311-318.

Oosterhof NN, Tipper SP, Downing PE. 2012a. Viewpoint (in)dependence of action representations: an MVPA study. J Cogn Neurosci. 24: 975-89.

Oosterhof NN, Tipper SP, Downing PE. 2012b. Visuo-motor imagery of specific manual actions: a multi-variate pattern analysis fMRI study. Neuroimage. 63: 262-71.

Oosterhof NN, Wiggett AJ, Diedrichsen J, Tipper SP, Downing PE. 2010. Surface-based information mapping reveals cross-modal vision–action representations in human parietal and occipitotemporal cortex. J Neurophysiol. 104: 1077–1089.

Pani P, Theys T, Romero MC, Janssen P. 2014. Grasping execution and grasping observation activity of single neurons in the macaque anterior intraparietal area. J Cogn Neurosci. 26: 2342–2355.

Perrett DI, Harries MH, Bevan R, Thomas S, Benson PJ, Mistlin AJ, Chitty AJ, Hietanen JK, Ortega JE. 1989. Frameworks of analysis for the neural representation of animate objects and actions. J Exp Biol. 146:, 87–113.

Pihko E, Nangini C, Jousmäki V, Hari R. 2010. Observing touch activates human primary somatosensory cortex. Eur J Neurosci. 31: 1836-43.

Platonov A, Orban GA. 2016. Action observation: the less-explored part of higher-order vision. Sci Rep. 6: 36742.

Popivanov ID, Jastorff J, Vanduffel W, Vogels R. 2012. Stimulus representations in body-selective regions of the macaque cortex assessed with event-related fMRI. Neuroimage. 63: 723-41.

Puce A, Perrett D. 2003. Electrophysiology and brain imaging of biological motion. Philos Trans R Soc Lond B Biol Sci. 358: 435-45.

Pulvermüller F, Fadiga L. 2010. Active perception: sensorimotor circuits as a cortical basis for language. Nat Rev Neurosci. 11: 351-360.

Raos V, Evangeliou MN, Savaki HE. 2004. Observation of action: grasping with the mind's hand. Neuroimage. 23: 193-201.

Raos V, Evangeliou MN, Savaki HE. 2007. Mental simulation of action in the service of action perception. J Neurosci. 27: 12675-83.

Raos V, Umiltá MA, Murata A, Fogassi L, Gallese V. 2006. Functional properties of grasping-related neurons in the ventral premotor area F5 of the macaque monkey. J Neurophysiol. 95: 709-729.

Raos V, Savaki HE. 2016a. Perception of actions performed by external agents presupposes knowledge about the relationship between action and effect. Neuroimage. 132: 261-273.

Raos V, Savaki HE. 2016b. The Role of the Prefrontal Cortex in Action Perception. Cereb Cortex. 27: 4677–4690.

Rizzolatti G, Camarda R, Fogassi L, Gentilucci M, Luppino G, Matelli M. 1988. Functional organization of inferior area 6 in the macaque monkey. II. Area F5 and the control of distal movements. Exp Brain Res. 71: 491-507.

Rizzolatti G, Fadiga L. 1998. Grasping objects and grasping action meanings: the dual role of monkey rostroventral premotor cortex (area F5). Novartis Found Symp. 218: 81-95.

Rizzolatti G, Fogassi L, Gallese V. 2001. Neurophysiological mechanisms underlying the understanding and imitation of action. Nat Rev Neurosci. 2: 661-670.

Rizzolatti G, Luppino G. 2001. The cortical motor system. Neuron. 31: 889-901.

Rizzolatti G, Sinigaglia C. 2016. The mirror mechanism: a basic principle of brain function. Nat Rev Neurosci. 17: 757–765.

Rochat MJ, Caruana F, Jezzini A, Escola L, Intskirveli I, Grammont F, Gallese V, Rizzolatti G, Umiltà MA. 2010. Responses of mirror neurons in area F5 to hand and tool grasping observation. Exp Brain Res. 204: 605–616.

Rozzi S, Coudé G. 2015. Grasping actions and social interaction: neural bases and anatomical circuitry in the monkey. Front Psychol. 6: 973.

Rozzi S, Ferrari PF, Bonini L, Rizzolatti G, Fogassi L. 2008. Functional organization of inferior parietal lobule convexity in the macaque monkey: electrophysiological characterization of motor, sensory and mirror responses and their correlation with cytoarchitectonic areas. Eur J Neurosci. 28: 1569–1588.

Saito N, Mushiake H, Sakamoto K, Itoyama Y, Tanji J. 2005. Representation of immediate and final behavioral goals in the monkey prefrontal cortex during an instructed delay period. Cereb Cortex. 15:1535-46.

Scangos KW, Aronberg R, Stuphorn V. 2013. Performance monitoring by presupplementary and supplementary motor area during an arm movement countermanding task. J Neurophysiol. 109: 1928-1939.

Sharma S, Fiave PA, Nelissen K. 2018. Functional MRI responses to passive, active and observed touch in somatosensory and insular cortices of the macaque monkey. J Neurosci. 38: 3689-3707.

Shima K, Mushiake H, Saito N, Tanji J. 1996. Role for cells in the presupplementary motor area in updating motor plans Proc Natl Acad Sci USA. 93: 8694-8698.

Simone L, Bimbi M, Rodà F, Fogassi L, Rozzi S. 2017. Action observation activates neurons of the monkey ventrolateral prefrontal cortex. Sci Rep. 7: 44378.

Simone L, Rozzi S, Bimbi M, Fogassi L. 2015. Movement-related activity during goal-directed hand actions in the monkey ventrolateral prefrontal cortex. Eur J Neurosci. 42: 2882–2894.

Stoianovici D, Patriciu A, Petrisor D, Mazilu D, Kavoussi L. 2007. A new type of motor: pneumatic step motor. IEEE ASME Trans Mechatron. 12: 98-106.

Tanji J. 2001. Sequential organization of multiple movements: involvement of cortical motor areas
Annu Rev Neurosci. 24: 631-651.

Tkach D, Reimer J, Hatsopoulos NG. 2007. Congruent activity during action and action observation in motor cortex. J Neurosci. 27: 13241-50.

Tootell RB, Reppas JB, Kwong KK, Malach R, Born RT, Brady TJ, Rosen BR, Belliveau JW. 1995. Functional analysis of human MT and related visual cortical areas using magnetic resonance imaging. J Neurosci. 15: 3215-30.

Vander Wyk BC, Voos A, Pelphrey KA. 2012. Action representation in the superior temporal sulcus in children and adults: an fMRI study. Dev Cogn Neurosci. 2: 409-16.

Vanduffel W, Fize D, Mandeville JB, Nelissen K, Van Hecke P, Rosen BR, Tootell RB, Orban GA. 2001. Visual motion processing investigated using contrast agent-enhanced fMRI in awake behaving monkeys. Neuron. 32: 565-577.

Vigneswaran G, Philipp R, Lemon RN, Kraskov A. 2013. M1 corticospinal mirror neurons and their role in movement suppression during action observation. Curr Biol. 23: 236–243.

Wurm MF, Lingnau A. 2015. Decoding actions at different levels of abstraction. J Neurosci. 35: 7727-35.

Yoshida K, Saito N, Iriki A, Isoda M. 2011. Representation of others' action by neurons in monkey medial frontal cortex. Curr Biol. 21: 249-53.

Zabicki A, de Haas B, Zentgraf K, Stark R, Munzert J, Krüger B. 2016. Imagined and Executed Actions in the Human Motor System: Testing Neural Similarity Between Execution and Imagery of Actions with a Multi-variate Approach. Cereb Cortex. 27: 4523-4536.

Zhao F, Wang P, Hendrich K, Ugurbil K, Kim SG. 2006. Cortical layer-dependent BOLD and CBV responses measured by spin-echo and gradient-echo fMRI: insights into hemodynamic regulation. Neuroimage. 30: 1149-1160.

10. Supplementary Material

Video
[Click here to download Video: Movie_S1.mp4](#)

Video

[Click here to download Video: Movie_S2.mp4](#)

Video
Click here to download Video: Movie_S3.mp4

Video

[Click here to download Video: Movie_S4.mp4](Movie_S4.mp4)